Atmosphere

Volume 14 Number 4 1976

Canadian Meteorological Society
Société Météorologique du Canada

Atmosphere

Volume 14 Number 4 1976

Contents

Continued on inside back cover

ISSN 0004-6973

Canadian Meteorological Societ
Société Météorologique du Canad

CALL FOR NOMINATIONS – 1976 AWARDS

Nominations are requested from members and Centres for the 1976 CMS Awards to be presented at the 1977 Annual Meeting. Four awards are open for competition: 1) the President's Prize for an outstanding contribution in the field of meteorology by a member of the Society; 2) the Prize in Applied Meteorology, for an outstanding contribution by a member in that field; 3) the Graduate Student Prize, for a contribution of special merit, and 4) the Rube Hornstein Prize in Operational Meteorology, for outstanding service in providing operational meteorological service. The awards will be made on the basis of contributions during the 1976 calendar year, except 4) which may be awarded also for work performed over a period of years.

Nominations are also requested for the award of citations to individuals or groups in Canada who have made some outstanding contribution in helping to alleviate pollution problems or in developing environmental ethics.

All nominations should reach the corresponding secretary not later than *1 February 1977*.

APPEL AUX CANDIDATURES POUR LES PRIX ET CITATIONS 1976

On demande aux membres et aux centres locaux de soumettre leurs nominations aux candidatures pour les prix de la Société pour l'année 1976. Il y a quatre prix: 1) le prix du président pour un travail exceptionnel en météorologie par un membre de la Société, 2) le prix de météorologie appliquée pour un travail exceptionnel dans ce domaine par un membre, 3) le prix aux étudiants gradués et 4) le prix de météorologie opérationnelle Rube Hornstein pour un travail exceptionnel dans l'exploitation des services météorologiques.

Tous les prix seront attribués pour un travail qui a été effectué durant l'année 1976, à l'exception de 4) qui peut aussi être attribué pour un travail effectué durant une période couvrant plusieurs années.

On demande aussi des nominations de candidats susceptibles de se voir décerner une citation par la Société. Une citation peut être décernée à un individu ou à un groupe qui a apporté une contribution exceptionnelle à la solution des problèmes de la pollution, à l'amélioration de l'environnement ou au développement d'une éthique écologique.

Toutes les nominations recueillies par le secrétaire-correspondant avant *le 1er février 1977* seront remises aux comités des récompenses et des citations, selon le cas.

On the Modelling of Stationary Planetary Waves[1]

Christiane Beaudoin[2]
and
Jacques Derome
Department of Meteorology, McGill University, Montréal H3A 2K6

[Original manuscript received 18 November 1975; in revised form 18 May 1976]

ABSTRACT

The structure of the atmospheric stationary planetary waves is obtained by means of the quasi-geostrophic linear model developed by Matsuno (1970). To show the influence of the upper boundary condition on the structure of the waves, the latter is computed using a rigid top and a radiation condition. The modifications to the wave structure obtained when the upper boundary is lowered from a height of 65 km to 42.5 km, 32.5 km, and 22.5 km are examined. The effects of varying the vertical grid increment are studied through a comparison of the wave structures obtained with 6, 12, and 24 levels between 5 and 65 km.

1 Introduction

Lindzen et al. (1968) have shown that the use of an energy reflecting upper boundary condition in simplified models of large scale atmospheric flow can lead to spurious resonance phenomena. Relatively little has been done, however, since then to determine whether more realistic atmospheric models are as sensitive to the formulation of the upper boundary condition as the one discussed by Lindzen et al. For example in models designed to simulate quasi-geostrophic motion, the use of a rigid top as an upper boundary condition would be justifiable if the atmosphere and its model have mechanisms that prevent any energy from reaching the boundary from below and if, of course, there are no energy sources above the upper boundary of the model. In particular, Matsuno's (1970) linear model of stationary planetary waves had such mechanisms, since very little energy reached the upper boundary at 65 km. It is evident then that the merits of a reflective upper boundary condition cannot be assessed without careful consideration of the ability of a model to prevent vertically propagating energy from reaching the upper boundary.

For obvious reasons of economy most models that are used for numerical weather prediction (e.g. Shuman and Hovermale, 1968) or for general circulation research (e.g. Manabe and Terpstra, 1974) have a much lower vertical resolution near the top of the model than the one used by Matsuno, or have

[1]Research supported by the National Research Council under grant A8613
[2]Now with the Atmospheric Environment Service of Canada

much lower tops (Kasahara et al., 1973). In such models it is not well known how much wave energy is spuriously reflected at the upper boundary and how the evolution of the model is affected by such reflection. Some information has been presented recently by Williams (1976) who has compared the structures of quasi-stationary planetary waves in two general circulation models with rigid tops, at 18 km in one model and at 36 km in the other. The results indicated that the presence of a rigid top at 18 km affected significantly the structure of the quasi-stationary waves. It was not clear, however, whether the rigid top had any serious effect on the waves when it was set at 36 km.

In the present study we shall examine how the formulation of the upper boundary condition and the height at which it is applied affects the structure of a forced stationary planetary wave. The wave structures obtained with a linear quasi-geostrophic model bounded above by a rigid top at various heights are compared with those obtained using a radiation condition in order to determine the sensitivity of the computed structure to the type of boundary condition used and the height at which it is applied. The dependence of the wave structure on the vertical grid length is also discussed.

2 The model

The model used in this study is the one described by Matsuno (1970) so that only a brief description will be presented here. Steady quasi-geostrophic small-amplitude perturbations are superimposed upon a basic state in which the zonal wind varies with latitude and height. When the vertical velocity is eliminated between the linearized vorticity and thermodynamic equations the following potential vorticity equation is obtained for zonal wave number m:

$$\frac{\sin^2\theta}{\cos\theta}\frac{\partial}{\partial\theta}\left(\frac{\cos\theta}{\sin^2\theta}\frac{\partial\psi_m}{\partial\theta}\right) + l^2\sin^2\theta\,\frac{\partial^2\psi_m}{\partial z^2} + Q_m\psi_m = 0 \qquad (1)$$

where $Q_m = \dfrac{\partial\bar{q}}{\partial\theta}\cdot\dfrac{1}{(\bar{\omega} - i\alpha/m)} - \dfrac{l^2\sin^2\theta}{4H_0{}^2} - \dfrac{m^2}{\cos^2\theta}$

$$\frac{\partial\bar{q}}{\partial\theta} = \left[2(\Omega + \bar{\omega}) - \frac{\partial^2\bar{\omega}}{\partial\theta^2} + 3\tan\theta\,\frac{\partial\bar{\omega}}{\partial\theta} - 4\Omega^2 a^2\sin^2\theta\,\frac{1}{p}\frac{\partial}{\partial z}\left(\frac{p}{N^2}\frac{\partial\bar{\omega}}{\partial z}\right)\right]\cos\theta$$

$$l = \frac{2\Omega a}{N}$$

$$\psi_m = e^{-(z-5)/2H_0}\,\phi_m/g$$

and where the other symbols have the following meaning:

θ latitude
z height in kilometres
p pressure
a earth's radius
Ω earth's rotation rate

$\bar{\omega}$ angular speed of the basic zonal flow
g gravity
$\bar{q}$ potential vorticity of the basic state
H_0 scale height, taken to be 7 km
N Brunt-Vaisala frequency, $2 \times 10^{-2} s^{-1}$
ϕ_m complex amplitude of zonal wave number one in the geopotential
α constant coefficient of Newtonian cooling and Rayleigh friction, $5 \times 10^{-7} s^{-1}$.

The geopotential $\phi_m(\theta)$ (and hence ψ_m) is specified at $z = 5$ km and the finite difference version of (1) with $\Delta\theta = 5$ degrees and $\Delta z = 2.5$ km (except where noted) is solved above 5 km subject to the boundary conditions $\psi_m(z, \theta = 0) = \psi_m(z, \theta = \pi/2) = 0$ and either a radiation condition (to be discussed in the next section) or a rigid top ($w' = dz/dt = 0$) boundary condition at $z = z_T$. When the radiation condition is used in the present study, α is assumed to have the same value above and below z_T. The basic state atmosphere is assumed to be isothermal above 5 km and the mean zonal wind distribution, $\bar{u} = \bar{\omega}\, a \cos\theta$, of Matsuno, which is reasonably typical of winter conditions is adopted in this study and is reproduced in Fig. 1.

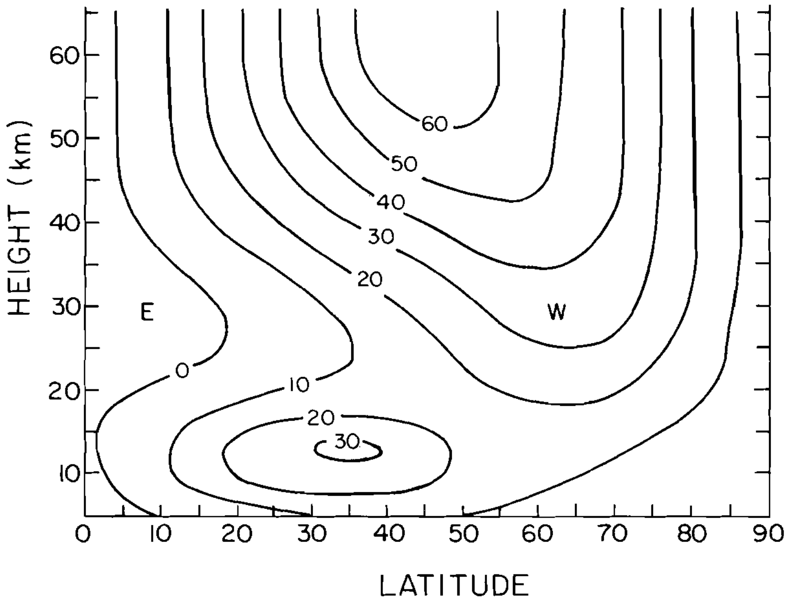

Fig. 1 Winter zonal wind distribution (m s^{-1}) redrawn from Matsuno (1970).

In the sequel, all results shown will apply to zonal wave number one, since the latter is known to penetrate higher into the upper stratosphere than the shorter waves and is consequently more likely to be affected by the choice of the upper boundary condition.

3 The radiation condition applied at various heights

The formulation of the radiation condition for the problem at hand has been described in detail by Matsuno (1970). To use it we divide the computational domain into two parts: the one below z_T where the mean zonal wind is a function of both latitude and height and the other from z_T to infinity where the mean zonal wind is independent of height. Above z_T (1) can be solved by the method of separation of variables. The horizontal structure equation, in which the separation constant is an eigenvalue, is solved numerically to obtain the various possible horizontal modes and corresponding eigenvalues. The vertical structure equation, a second order differential equation, is then solved analytically, and for each previously determined eigenvalue two possible solutions are obtained. Only those solutions that have a finite energy density at infinity and have either a vanishing or upward energy flux are retained as physically valid. The matching of a linear combination of these solutions in the region $z > z_T$ to the numerical solution below z_T then effectively provides the required upper boundary condition for the region $z < z_T$. Although in the following we shall refer to the radiation condition as having been applied "at z_T", it should be realized that strictly speaking it is the *matching* that is done at z_T and that a solution can be computed for all values of z. For simplicity only the part of the solution below z_T will be shown.

The wave structure obtained with the radiation condition applied at 65 km is shown in Fig. 2. The value of n in the caption gives the number of horizontal levels in the region 5 km $< z \leqslant z_T$. As expected, it is essentially the same as

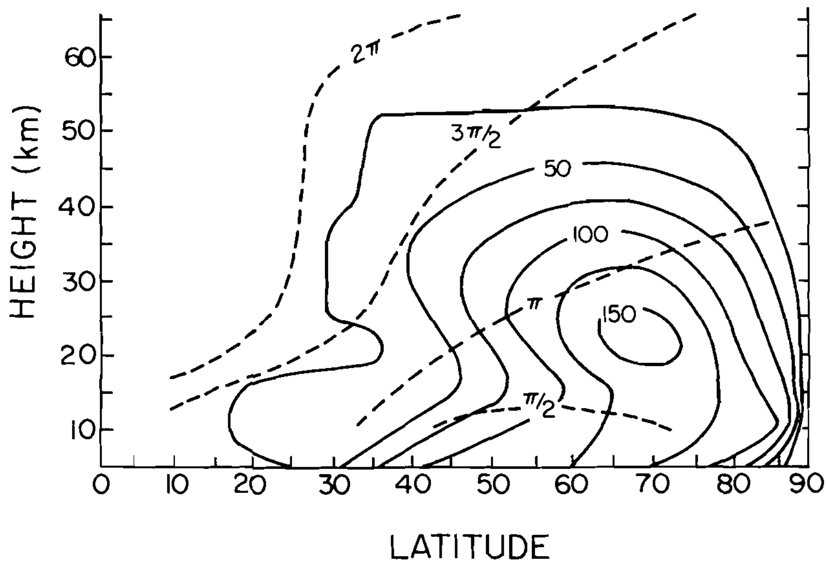

Fig. 2 Computed distribution of the amplitude of ψ (solid lines) in metres and its phase (dashed lines) in radians west of Greenwich, with the radiation condition applied at 65 km, $n = 24$.

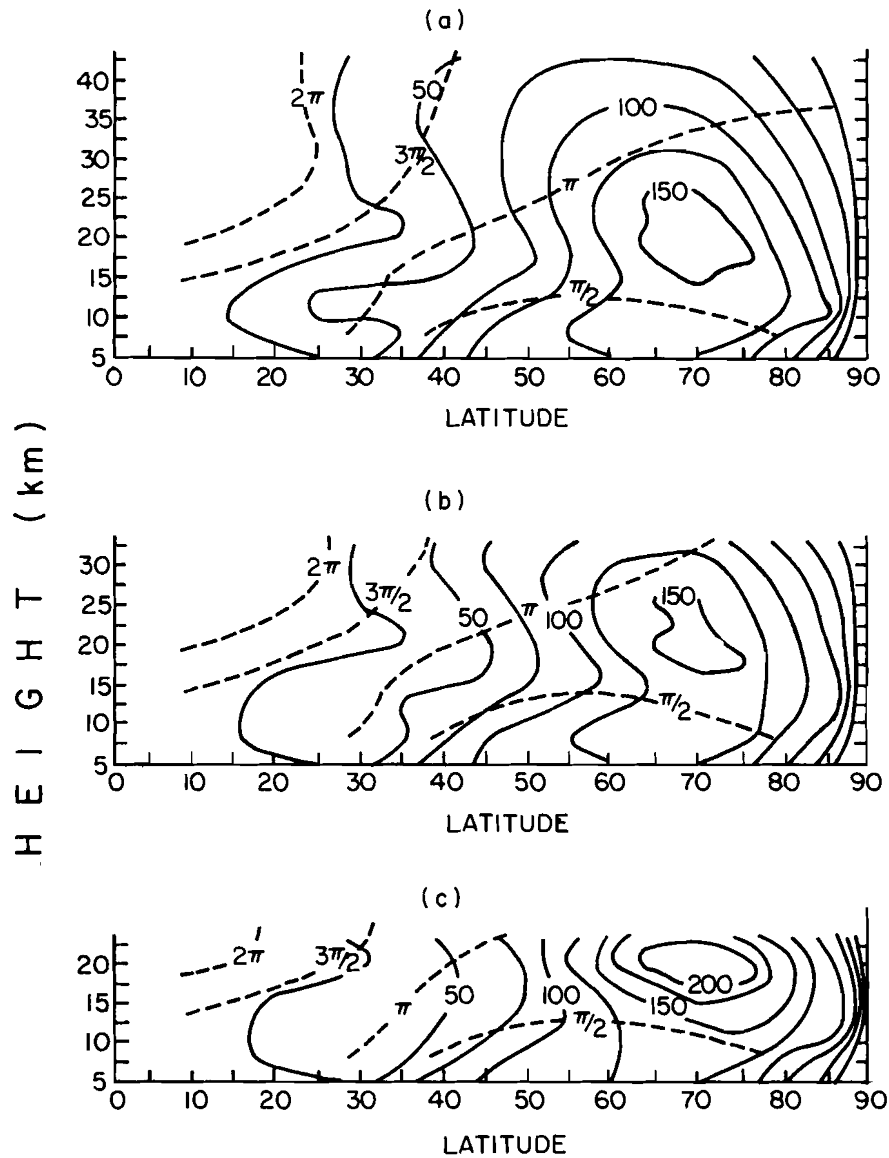

Fig. 3 Same as Fig. 2 except that the radiation condition is applied at (a) 42.5 km, $n = 15$; (b) 32.5 km, $n = 11$; (c) 22.5 km, $n = 7$.

Matsuno's Fig. 5(a) for the same case and it is being presented here simply to facilitate the discussion of subsequent results. When the radiation condition is applied at 42.5 km, 32.5 km, and then at 22.5 km the results of Fig. 3 are obtained. We see that there is a rather good agreement between Figs. 2, 3(a), and 3(b), as might have been anticipated since over most of the domain above 32.5 km ϖ is nearly independent of height (Fig. 1). These three cases, then, are based on very similar zonal wind distributions (recall that when the radiation condition is used, $\bar{\omega}$ is kept independent of z above z_T) and it is therefore not too surprising to see that they yield similar wave structures. When the radiation condition is applied at 22.5 km the computed wave structure is as shown in Fig. 3(c). The maximum value of the amplitude at 20 km and 70°N now reaches 224 m as compared to only 171 m when the boundary condition is applied at 65 km. Clearly the assumption that $\partial\bar{\omega}/\partial z$ above z_T leads to unsatisfactory results when z_T is set as low as 22.5 km and the "true" zonal wind distribution is as shown in Fig. 1.

4 A rigid top at various heights

When the rigid top boundary condition is applied at 65 km, the computed wave structure is essentially the same as that of Fig. 2 (Matsuno, 1970). On the other hand, when the rigid top is lowered to 42.5 km, 32.5 km, and 22.5 km, the wave structure becomes progressively more distorted as shown in Fig. 4. For example, when the rigid top is set at 32.5 km the maximum amplitude in the ψ_m field is larger than when the top is at 65 km and appears at 65°N and 25 km rather than at 70°N and 17.5 km. When the top is set at 22.5 km, however, a dramatic change in the wave structure occurs, showing the presence of a spurious resonance phenomenon. The results in this case are clearly unacceptable.

5 Vertical resolution

To determine the sensitivity of the results to the vertical resolution some computations were made with vertical grid increments of 5 and 10 km rather than 2.5 km as previously. The radiation condition was applied at 65 km. We can see from a comparison of Fig. 5(a), which gives the wave structure for the case $\Delta z = 5$ km, and Fig. 2, which is the control case with $\Delta z = 2.5$ km, that a grid increment of 5 km is sufficient to reproduce rather well the major features of the higher resolution results. The maximum amplitude of 161 m is now situated at a height of 20 km as opposed to the maximum of 171 m at 17.5 km in Fig. 2. The difference between the two phase angle distributions is insignificant.

When the vertical resolution is further reduced to $\Delta z = 10$ km the results of Fig. 5(b) are obtained. The maximum amplitude is now reduced to slightly more than 125 m and appears at 25 km. Again the phase angle is not seriously affected by a reduction in the vertical resolution. It appears, then, that while a vertical grid interval of 2.5 km may be somewhat finer than strictly necessary to resolve the structure of planetary waves in the stratosphere, an interval of 10 km will yield results that are significantly affected by the lack of resolution. It should be understood here that the discrepancies between Fig. 5(b) (or a) and Fig. 2 reflect both the greater truncation errors introduced by the increase in Δz and the fact that the low-resolution grid cannot resolve all the salient features of the mean zonal wind distribution.

It is interesting at this point to compare the results of Fig. 3(c) and Fig. 5(b) both of which are based on roughly the same number of computational levels,

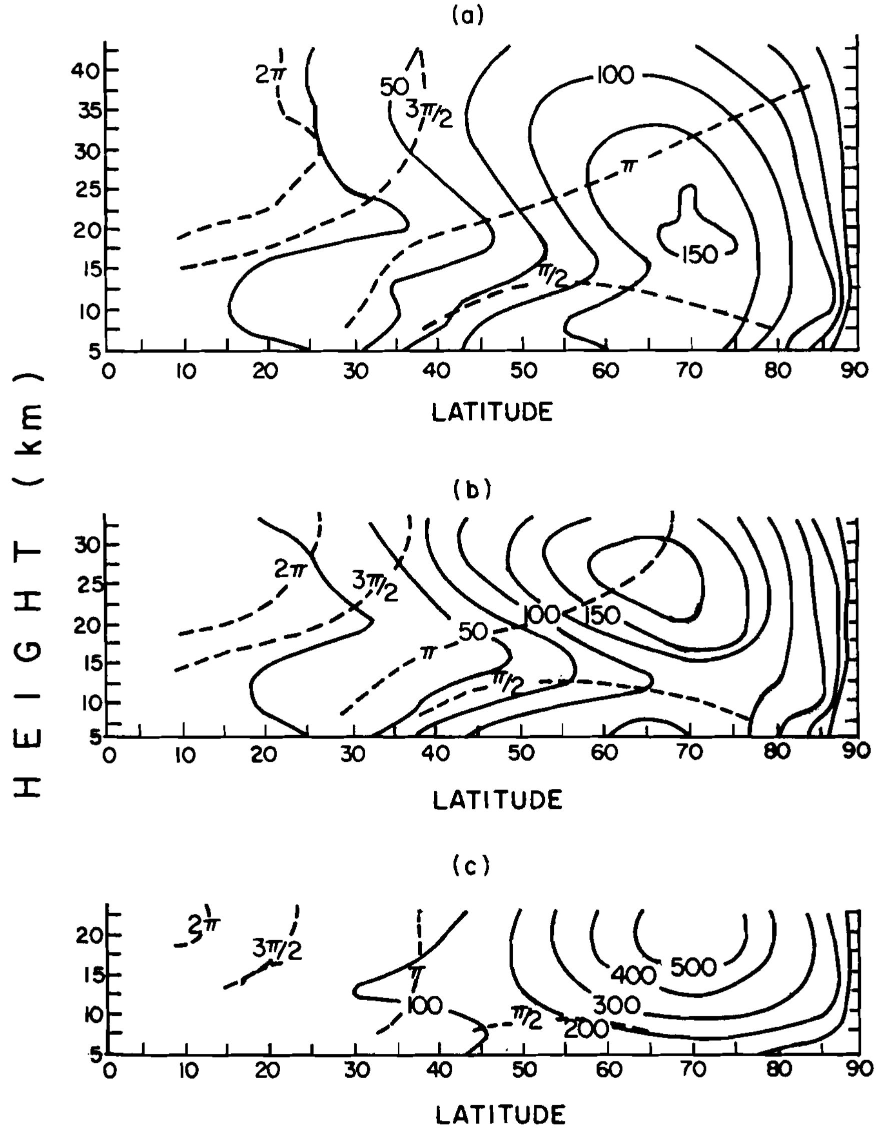

Fig. 4 Same as Fig. 2 except that the rigid top boundary condition is applied at (a) 42.5 km, $n = 15$; (b) 32.5 km, $n = 11$; (c) 22.5 km, $n = 7$.

n^*. The comparison shows that when ψ_m is computed at a relatively small number of levels, more realistic results are obtained when these few levels are spread over a deeper region of the stratosphere rather than concentrated in

*Although with the radiation condition it is possible to compute the solution for $z > z_T$ it is not necessary to do so and the computational effort required to obtain the solution in the region 5 km $< z \leqslant z_T$ is dependent on n.

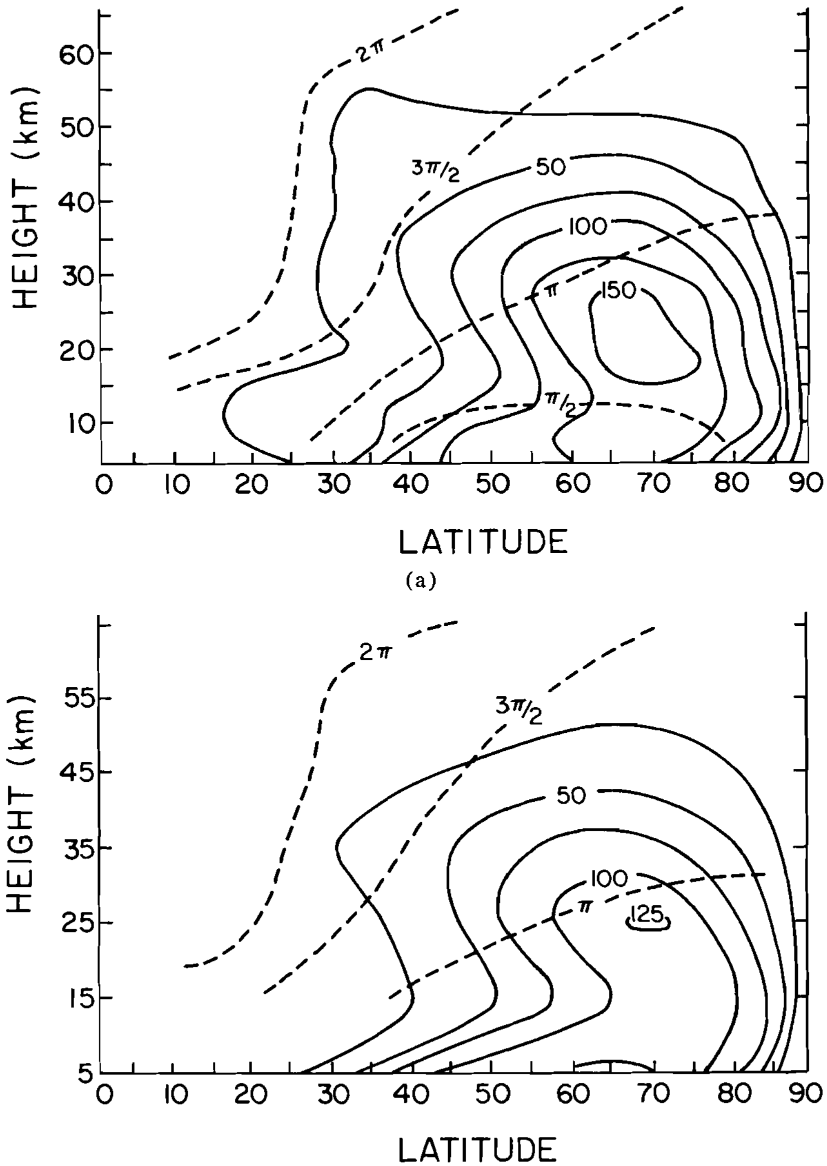

Fig. 5 (a) Same as Fig. 2 but with a vertical grid increment of 5 km, so that $n = 12$. (b) Same as Fig. 2 but with a vertical grid increment of 10 km, so that $n = 6$.

the lower layers. It appears then that the assumption $\partial\bar{\omega}/\partial z = 0$ for $z \geqslant 22.5$ km in Fig. 3(c) has more detrimental effects on the wave structure than the decrease in resolution in Fig. 5(b). A similar comparison cannot be made for the model with the rigid top boundary condition since the low-resolution case ($\Delta z = 5$ or 10 km, $z_T = 65$ km) has not been computed. Considering the very poor results obtained when the rigid top is located at 22.5 km, it seems likely that an improvement would be obtained if, for the same number of horizontal levels, the rigid top were raised to 65 km.

6 Conclusion

This study on the modelling of atmospheric stationary quasi-geostrophic long waves was focused on the influence of the upper boundary condition on the stratospheric structure of the waves. Attention was concentrated on zonal wave number one since it is known to propagate vertically more freely than shorter waves and is more likely to be affected by the formulation of the upper boundary.

Using a linearized quasi-geostrophic model with a zonal wind distribution which is fairly typical of winter conditions, it was found that while the radiation upper boundary condition and the rigid top condition yield similar results when both applied at 65 km, they yield drastically different results when applied at 22.5 km. In this case the radiation condition yields a wave structure which, while being rather different from the one obtained when the upper boundary is at 65 km, is nevertheless superior to the solution obtained with a rigid top at 22.5 km. In fact, a rigid top at 22.5 km yields completely meaningless results for the wave structure in the lower stratosphere.

A comparison of the wave structures obtained using the radiation boundary condition with (a) 7 horizontal levels between 5 and 22.5 km and (b) 6 levels between 5 and 65 km, revealed that (b) yields better results even though the vertical grid increment is four times larger. It appears that the conclusion would be qualitatively the same if a rigid top boundary condition were used.

It should finally be emphasized that the results described in this study apply to a specific zonal wind distribution. Different results might be obtained, for example, with a summer zonal wind distribution.

References

CHARNEY, J.G. and P.G. DRAZIN. 1961. Propagation of planetary-scale disturbances from the lower into the upper atmosphere. *J. Geoph. Res.* **66**: 83–109.

KASAHARA, A.; T. SASAMORI; and W.M. WASHINGTON. 1973. Simulation experiments with a 12-layer stratospheric global circulation model. I Dynamical effect of the earth's orography and thermal influence of continentality. *J. Atmos. Sci.* **30**: 1229–51.

LINDZEN, R.S.; E.S. BATTEN; and J.W. KIM. 1968. Oscillations in atmospheres with tops. *Mon. Wea. Rev.* **96**: 133–40.

MANABE, S. and T.B. TERPSTRA. 1974. The effects of mountains on the general circulation of the atmosphere as identified by numerical experiments. *J. Atmos. Sci.* **31**: 3–42.

MATSUNO, T. 1970. Vertical propagation of stationary planetary waves in the winter northern hemisphere. *J. Atmos. Sci.* **27**: 871–83.

SHUMAN, F.G. and J.B. HOVERMALE. 1968. An operational six-layer primitive equation model. *J. Appl. Meteor.* **7**: 525–47.

WILLIAMS, J. 1976. Zonal harmonic standing waves in the NCAR global circulation model. *Mon. Wea. Rev.* **104**: 249–59.

Scaling Turbulence in the Planetary Boundary Layer

G.A. McBean
Atmospheric Environment Service, Downsview, Ontario

[Manuscript received 14 January 1976; in revised form 10 August 1976]

ABSTRACT

Two different approaches to scaling turbulence in the planetary boundary layer over Lake Ontario are investigated. The height up to the inversion was found to be the appropriate scaling height while u_* for near-neutral and w_* for unstable conditions were the appropriate scaling velocities. The results were in general agreement with the numerical models of Deardorff (1972) and Wyngaard, Cote, and Rao (1974).

1 Introduction

One characteristic that distinguishes the planetary boundary layer (pbl) from the atmosphere above it is the almost continuous distribution in space and time of turbulent motion. The turbulence is responsible for the transfers of momentum, heat, and matter, for the bouncing of an aircraft on ascent or descent, and for the buffetting of tall structures. Although a comprehensive theory of the pbl is lacking, much progress has been made in numerically modelling the pbl (e.g. Deardorff, 1973). There is still a need, however, for experimental data against which these models can be compared. The data are also valuable for the development of empirical relationships, which are very useful for practical applications.

In this paper an analysis of data collected during the International Field Year on the Great Lakes (IFYGL) is presented. The turbulence data were obtained by the National Aeronautical Establishment T-33 jet aircraft, specially instrumented for turbulence measurements, and have been described by McBean and MacPherson (1976) and McBean and Paterson (1975). The buoy and radiosonde data were collected as part of the IFYGL basic data set and are available from the IFYGL data banks. It is proposed to consider the scaling of the turbulence as a function of height and stability. First, two possible scaling schemes for pbl turbulence will be described. Then a comparison of the two schemes will be presented and, finally, some empirical formulas will be given in the hope that they will be useful in some applications. The results will be compared, as well, with the numerical model results of Wyngaard, Cote, and Rao (1974; hereafter cited as WCR) and Deardorff (1972; hereafter cited as D72).

2 Turbulence scaling parameters

Although there are many possible ways of scaling turbulence, only the two most widely used will be considered. To represent the turbulence the standard deviations of the fluctuations of the three velocity components and virtual temperature and the fluxes of momentum and virtual heat will be used. The scaling will then be in non-dimensional form, i.e.

$$\sigma_x/P_x = G_x(z/P_z, S)$$

and

$$F_x/D_x = C_x(z/P_z, S)$$

where σ_x is the standard deviation of the fluctuations of x,
F_x is the flux of x,
D_x, P_x, P_z are the scaling parameters,
z is the height
S is the stability
and G_x, C_x are unknown functions which will be different for each x.

For each scaling scheme we need a scaling velocity, a scaling temperature, a scaling height, and a non-dimensional number to represent stability. Because there is some latitude in choosing these scales it is necessary to consider the physical basis for the scaling. In analogy with surface-layer scaling (see, e.g. Wyngaard, 1973) we can use for scaling velocity and temperature:

$u_* = \{\tau/\rho\}^{1/2}$ where τ is the surface stress,
$T_* = -Q/u_*$ where Q is the virtual temperature flux;

and for stability, a height divided by the Monin-Obukhov length, $L = u_*^2T/kgT_*$ where k is von Kármán's constant ($= 0.4$). For the neutral barotropic pbl the relevant scaling height is cu_*/f (Tennekes, 1973), where f is the magnitude of the Coriolis parameter and c is an undetermined constant with a value between 0.2 and 0.5.

For convective conditions an alternate surface layer scaling is:

$$u_f = (zgQ/T)^{1/3}$$
$$T_f = (Q^2T/gz)^{1/3}$$

Deardorff (1973) has found for unstable conditions that u_*/f was not a relevant height and that h, the depth of the unstable layer under the inversion, was more pertinent. Then, pbl scaling velocities and temperatures are

$$w_* = (hgQ/T)^{1/3}$$

and

$$\theta_* = (Q^2T/gh)^{1/3}.$$

We thus have two sets of scaling parameters as summarized in Table 1. Note that all the parameters are independent of height since they are defined in terms of the surface stress and heat flux and the height of the inversion. T is a representative temperature of the layer. It should also be noted that these simple scaling schemes may be an oversimplification. For second-order effects more complicated schemes will likely be needed.

TABLE 1. Two possible sets of scaling and stability parameters

	(a)	(b)
velocity	u_*	w_*
temperature	T_*	θ_*
height	cu_*/f	h
stability	cu_*/fL	h/L

The bulk transfer equations

$$u_*^2 = C_D \bar{u}_{10}^2$$

$$Q = C_D \bar{u}_{10}((T_w - T_a) + 0.61T(q_* - q_a))$$

$$C_D = (0.58 + 0.068\bar{u}_{10}) \times 10^{-3} \qquad (\bar{u} \text{ in m s}^{-1}; \quad \text{Smith, 1973})$$

were used to compute the surface stress and vertical heat flux, as in McBean and Paterson (1975). The height of the inversion was determined by examining the radiosonde data around the lake and deducing what the profile over the lake would look like. There is a considerable amount of subjectivity in determining h and the errors could be significant.

3 Results

The observations were made on 8, 9, 12 and 15 October 1972 and only flight legs over the lake are considered. Most of the flights (43) were flown 150 m above the lake with some at 30 m (5), 60 m (8), and 300 m (7) for a total of 63 flights. The flights were generally 45 km (6 min at 125 m s^{-1}) in length and were flown at various angles to the mean wind. On all days there was scattered-to-broken cumulus and stratocumulus clouds. Cloud bases were generally 800–1500 m above the surface and often within the boundary layer. All flights were flown well below cloud bases. In order to separate the effects of stability from those of height the data were divided into stability groups dependent on either cu_*/fL or h/L (Table 2). The number of groups for h/L was smaller because the stability variations were expected to be smaller.

In Fig. 1 the heights h and 0.5 u_*/f are compared. For Group A the points scatter but most fall near the line $h \sim 0.3\ u_*/f$. The points in the lower right sector were for cases of significant baroclinicity. For Group C the points are near $h \sim 0.5\ u_*/f$ with the points for Group B being intermediate. The D72

TABLE 2. Stability classifications

$0.5u_*/fL$			h/L		
Group	Range	No. of Obs	Group	Range	No. of Obs
I	0:−10	17	A	0:−12	33
II	−10:−20	16	B	−12:−34	11
III	−20:−40	11	C	−34:−65	19
IV	−40:−50	12			
V	−50:−70	7			

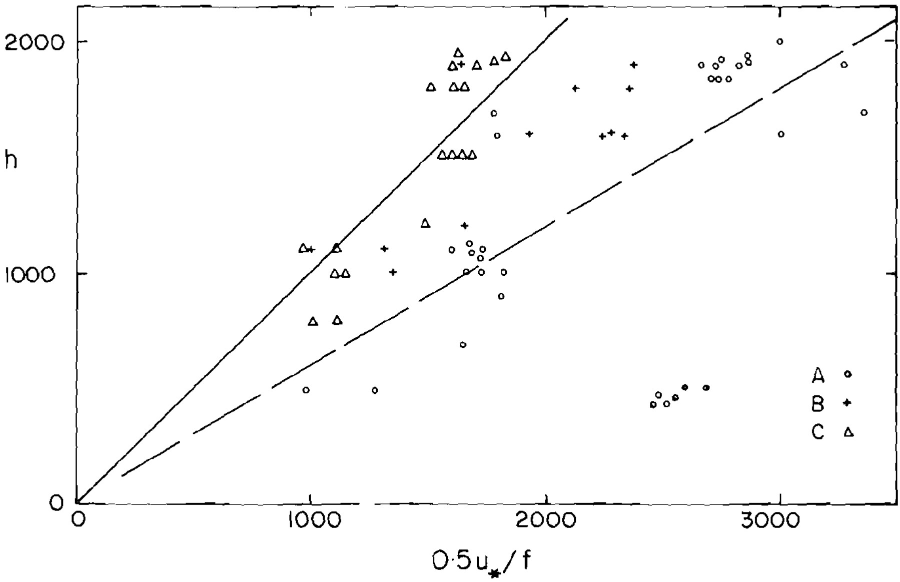

Fig. 1 The relationship between the height up to the inversion, h, and the dynamic height, $0.5\ u_*/f$, for each of the three stability groups A, B, C. The solid line is $h = 0.5\ u_*/f$ and the dashed line is $h = 0.3\ u_*/f$.

modelling studies indicate that h is not related to u_*/f. Both D72 and WCR found the height of the momentum boundary layer for the neutral case to be $0.3\ u_*/f$. Since h is the height of the thermal boundary layer and is poorly defined for near neutral conditions, it may be only coincidental that $h \sim 0.3\ u_*/f$ was found here for Group A.

Vertical velocity fluctuations

In order to objectively determine which scaling gave the best fit to the data, the following procedure was used. Each variable was non-dimensionalized with either u_*, w_*, etc. and plotted against z/h or zf/cu_* for each stability group. Then polynomials (up to order 3) were fitted by the method of least squares and the scaling scheme that most reduced the variance was accepted as best. For Group I the best approach was σ_w/u_* vs z/h. For each of Groups II to V, σ_w/w_* vs z/h was as good or better than any other scheme. This result was expected and is in agreement with D72. An advantage of the σ_w/w_* vs z/h scaling is that the stability dependence of the relationship was negligibly small. h was the most appropriate scaling height in all cases so it seems more appropriate to look at stability groupings A, B, C. It was found that w_* and h scaling was most appropriate for all three stability groupings. The reduction in variance by grouping on basis of h/L was generally better than the groupings based on cu_*/fL.

It is somewhat surprising that w_* and h proved to be the better scaling system for Group A. It was expected that u_* and u_*/f scaling would be more appropriate for the near neutral cases. Clarke and Hess (1973) found for the Wangara mean wind and temperature profiles that u_*/f scaling was better than h for all cases. To investigate the effects near neutral, those cases with $-h/L < 3$ were considered separately. The scaling combination (w_*, h) was again the best. The ratios of the standard deviation from the best-fit, third-order polynomial to the standard deviation from the mean were: (w_*, h), 0.41; (u_*, u_*/f), 0.64; (u_*, h), 0.79; and (w_*, u_*/f), 0.84. It should be noted that ten of the twelve cases in this subgroup had h/L values between 2 and 3 and for all cases $z < L$. Surface layer measurements (McBean, 1971; Wyngaard, 1973) have shown the onset of local free convection for $z \sim |0.4L|$. Seven of the twelve cases in this subgroup have $z > |0.4L|$ and hence local free convection is possible. Because of the small number of cases, it is not possible to further subdivide the data. The energy input by buoyancy affects most directly the vertical velocity and temperature fluctuations. This may be the reason why these data scale better with (w_*, h) while Clarke and Hess found (u_*, u_*/f) preferable.

In Fig. 2 the variations of σ_w/u_* (Group A) and σ_w/w_* (all Groups) with z/h are shown. There is no difference between the Groups for h/L scaling. WCR found no variation of σ_w/w_* with h/L for $-50 < h/L < -10$ but their results for σ_w/w_* and those of D72 are larger than those presented here.

Horizontal velocity fluctuations

The velocity fluctuations in the longitudinal, u, and lateral, v, directions did not scale as well as the vertical velocity fluctuations. This characteristic has been observed in most other studies and can be attributed to the effects of large scale spatial or temporal inhomogeneities that are not accounted for in the scaling schemes. For the longitudinal component (u_*, h) was best for Groups I and A although (u_*, u_*/f) also gave good results. For the more unstable groups (w_*, h) was the preferable scheme. For the lateral component, the results were not as consistent and the scaling frequently did not reduce the variance to the level of 1% significance (Brooks and Carruthers, 1953, p. 303). For Group A (w_*, h) was best and for Group B (w_*, h) and (u_*, h) equal. For Group C no scheme was statistically significant.

In Figs 3 and 4 the scaled results for σ_u and σ_v are given. For Group A the results, scaled by (u_*, h), are quite scattered with an indication of a decrease in σ_u and σ_v with z/h increasing. The model computations of D72 and WCR bracket most of the data points, except for z/h near 0.35 where there are several measured values of both σ_u and σ_v that seem too large. There are also two cases for $z/h \sim 0.09$ with large values; these were for adjacent flight legs and it appears that the surface wind estimate is anomalously low.

For the unstable group (Groups B and C together) there is the same amount of scatter with a slight increase of σ_u/w_* and σ_v/w_* with z/h. The results are in approximate agreement in magnitude with D72 and WCR. However, since the D72 model predicts a decrease with z/h and the WCR model predicts an increase, a detailed comparison is not worthwhile.

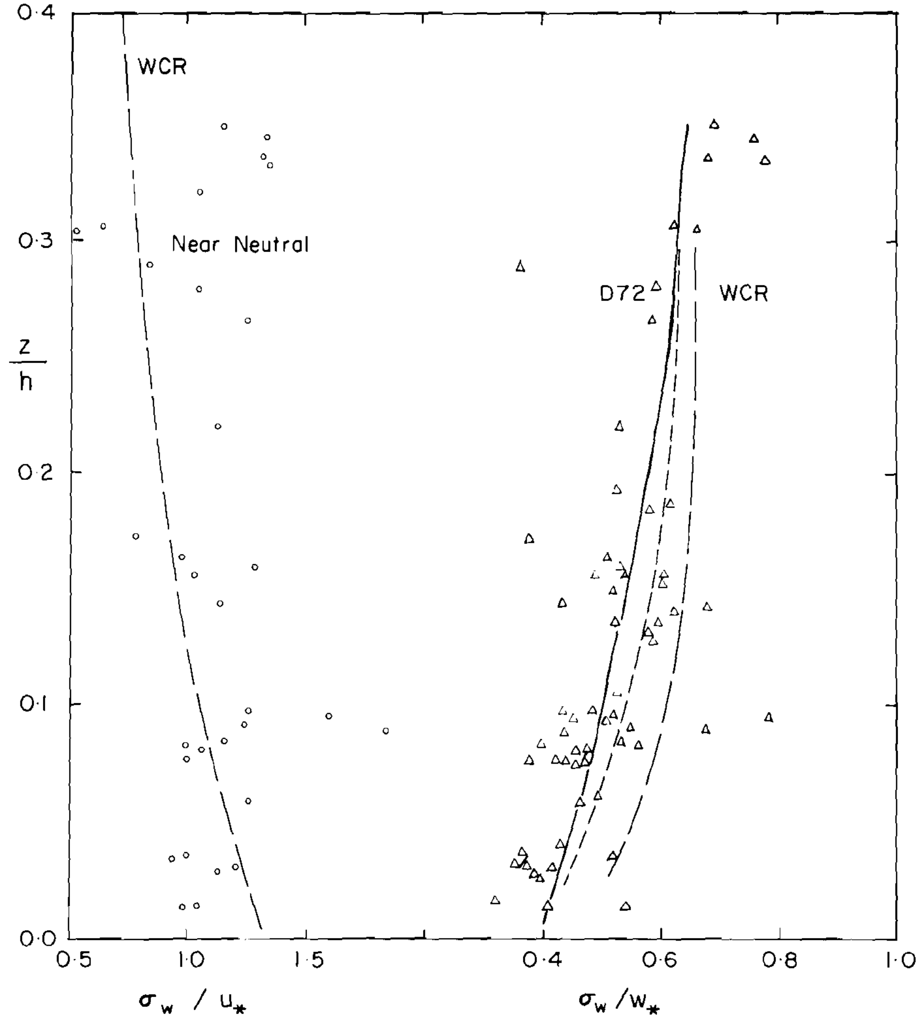

Fig. 2 Non-dimensional standard deviations of vertical velocity fluctuations against the non-dimensional height, z/h. On the left are the near-neutral data (Group A), non-dimensionalized with u_*; on the right are the data non-dimensionalized with w_*. The WCR curve at the left is for $h/L = 0$, at the right $h/L = -50$ and the D72 curve is for $h/L = -45$. The solid curve on the right is $\sigma_w/w_* = 0.40 + 1.1\ z/h - 1.1\ (z/h)^2$.

Virtual temperature fluctuations

The virtual temperature fluctuations, θ_v, were not measured directly but can be related to temperature, θ, and humidity, q', fluctuations by,

$$\theta_v = \theta(1 + 0.61\bar{q}) + 0.61q'T - 0.61\overline{q'\theta}$$

The variance is then

$$\overline{\theta_v^2} = \overline{\theta^2}\,(1 + 0.61\bar{q})^2 + (0.61T)^2\,\overline{q'^2} + 2\,(1 + 0.61\bar{q})\ 0.61T\,\overline{\theta q'} + 0.37\,(\overline{q'\theta})^2$$

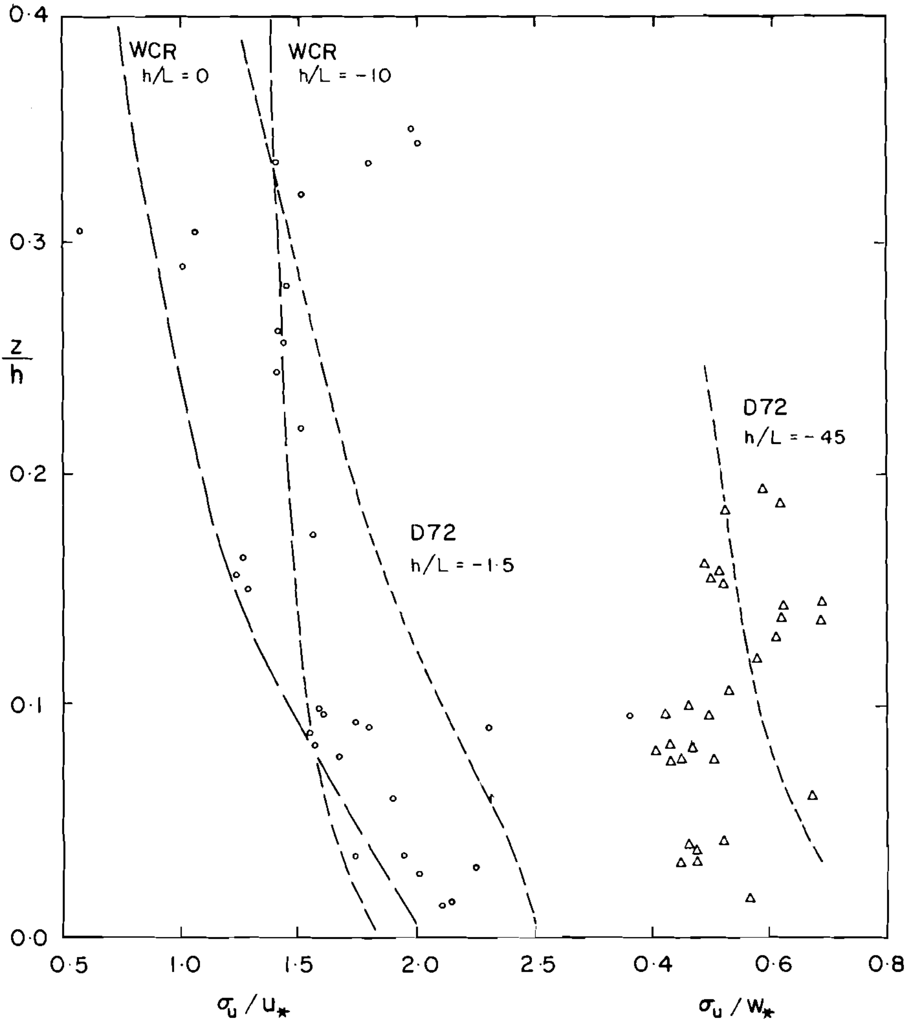

Fig. 3 Non-dimensional standard deviations of longitudinal velocity fluctuations against the non-dimensional height, z/h. On the left are the near-neutral data (Group A), non-dimensionalized with u_*; on the right are the unstable data (Groups B and C), non-dimensionalized with w_*. The WCR and D72 curves are for the stabilities indicated.

The fourth term can be shown to be neglible in comparison to the others. The other three terms are of the same order. However, the correlation $\overline{\theta q'}$ was not computed in the data processing. Therefore, the results to be presented are for

$$\sigma_{\theta_v} = \sigma_\theta(1 + 0.61\bar{q}) + 0.61T\sigma_q$$

and hence may be about 30% underestimated. The variations with height and stability, however, should not be greatly affected.

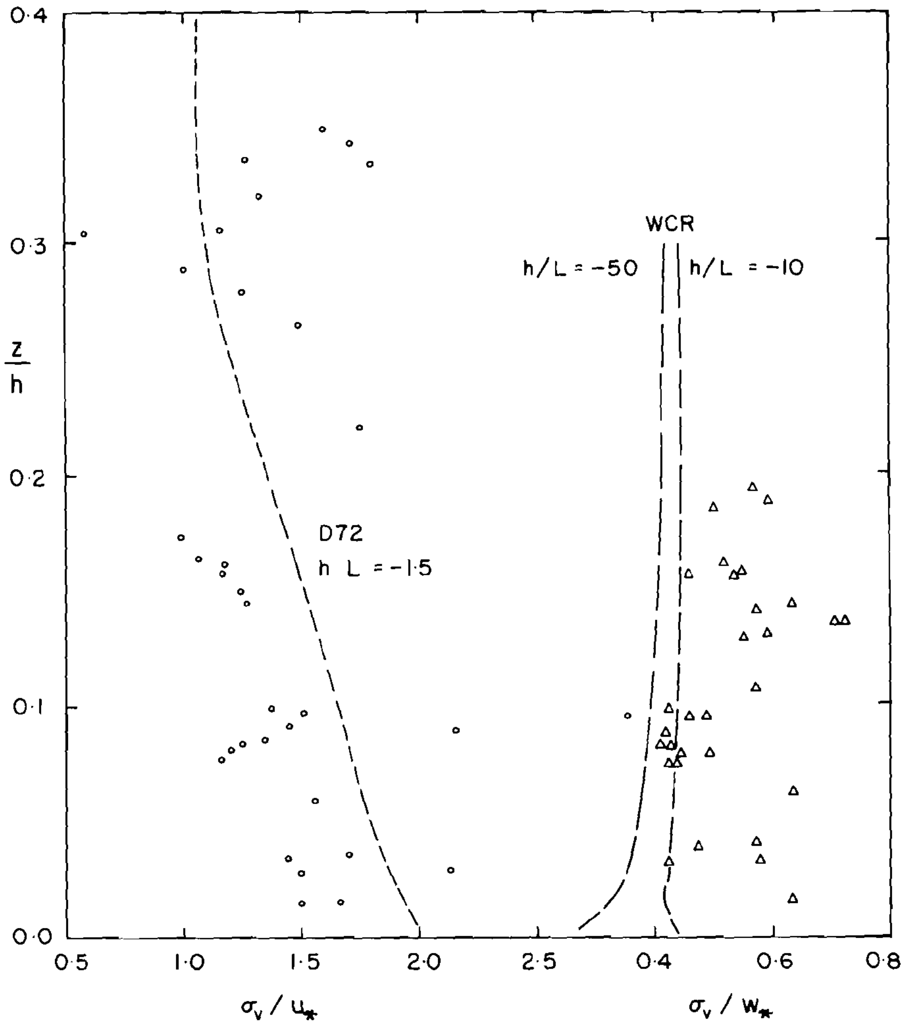

Fig. 4 Non-dimensional standard deviations of lateral velocity fluctuations against the non-dimensional height, z/h. (See Fig. 3).

For the near neutral group the data were quite scattered because of relatively low magnitudes for σ_{θ_v}, θ_* and T_*. For the unstable groups, h and θ_* are the best scaling parameters. The results (Fig. 5) show an increase of $\sigma_{\theta_v}/\theta_*$ with increasing z/h and are in reasonable agreement with D72 and WCR.

Momentum flux

The momentum flux is one of the most difficult variables to measure experimentally. The results here were no different. The data showed a large amount of scatter regardless of the scaling scheme. The scatter may be due to baroclinic effects and entrainment of air from above $z = h$, as discussed by Deardorff

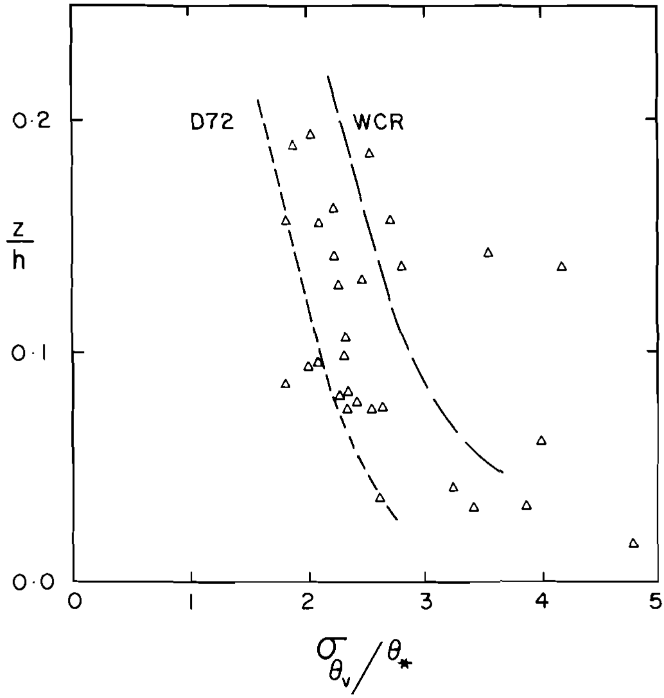

Fig. 5 Non-dimensional standard deviations of potential temperature fluctuations against the non-dimensional height, z/h, for the unstable Groups B and C. The WCR and D72 curves are for $h/L = -50$ and -45, respectively.

(1973). In Fig. 6 is $\overline{uw}/u_*^2$ vs z/h for Group A. For comparison, the model results of WCR for $h/L = 0$, -2 and -10 are shown. All that can be said is that the results do not disagree significantly. For the unstable groups the data are very scattered and not shown. The $\overline{vw}/u_*^2$ term was generally very small for small z/h and increased with z/h. The amount of scatter was again very large.

Virtual heat flux

The virtual heat flux can be computed as

$$\overline{w\theta_v} = \overline{w\theta}\,(1 + 0.61\bar{q}) + 0.61T\,\overline{wq'}$$

because the third order terms can be shown to be negligible. The virtual heat fluxes were very small for the near-neutral group and the ratio $\overline{w\theta_v}/Q$ decreased from near unity at $z/h = 0$ to 0 about $z/h \sim 0.3$ as shown in Fig. 7a. The shape is similar to that for momentum flux and indicates that the momentum and heat flux boundary layers are similar in depth ($z \sim 0.3\,h$). For Groups B and C (Fig. 7b), the data were also quite scattered. The best-fit straight line for Group C ($\overline{w\theta_v}/Q = 0.76 - 0.99\,z/h$, $r_{xy} = 0.32$) is shown. A second order

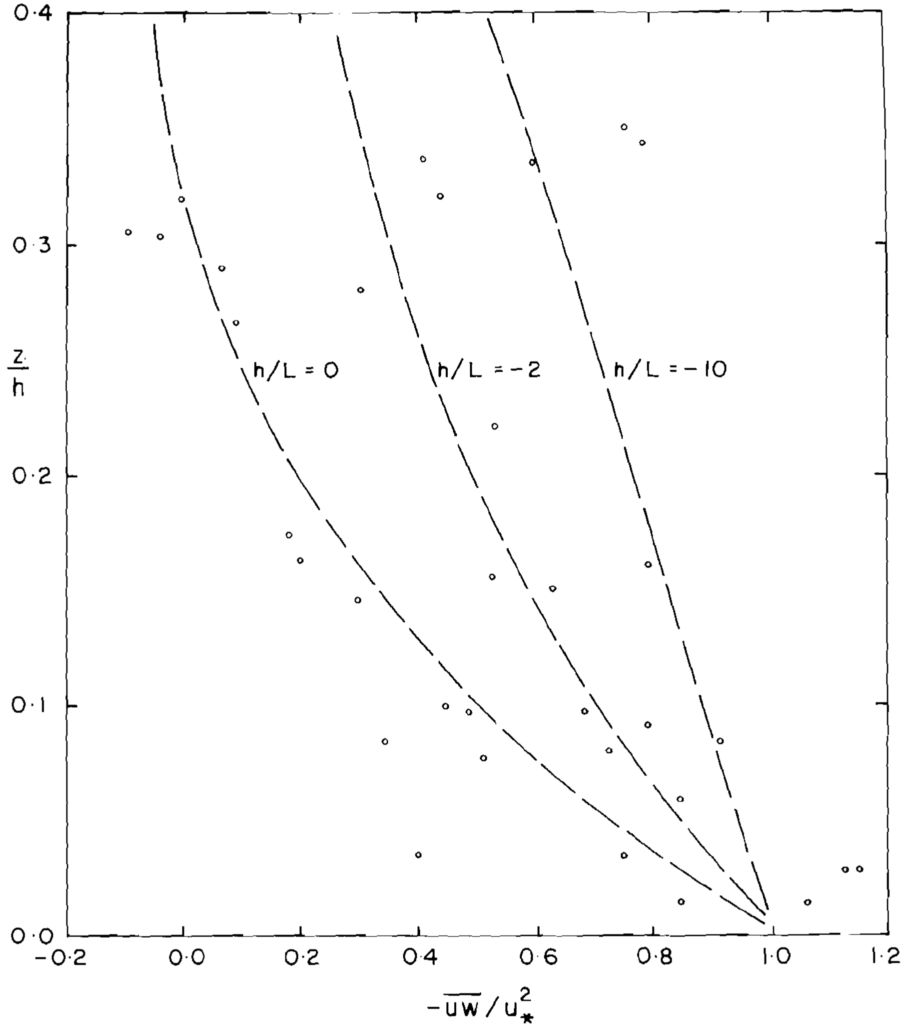

Fig. 6 Non-dimensional momentum flux or stress against the non-dimensional height z/h for the near-neutral Group A. The three dashed curves are all from WCR for the stabilities indicated.

polynomial fit did not significantly reduce the variance. When the analysis was done on Groups I to V it was found that linear fits had relatively high correlations for Groups I, II, and V. Extrapolations to $\overline{w\theta_v}/Q = 0$ gave values $z/h =$ 0.14 (Group I), 0.37 (Group II) and 0.68 (Group V). Thus, it seems that the heat flux boundary layer becomes deeper and approximates the height up to the inversion layer for unstable conditions. Lenschow (1970) found the heat flux equal to zero near $z/h = 0.8$ from measurements in an unstable boundary layer.

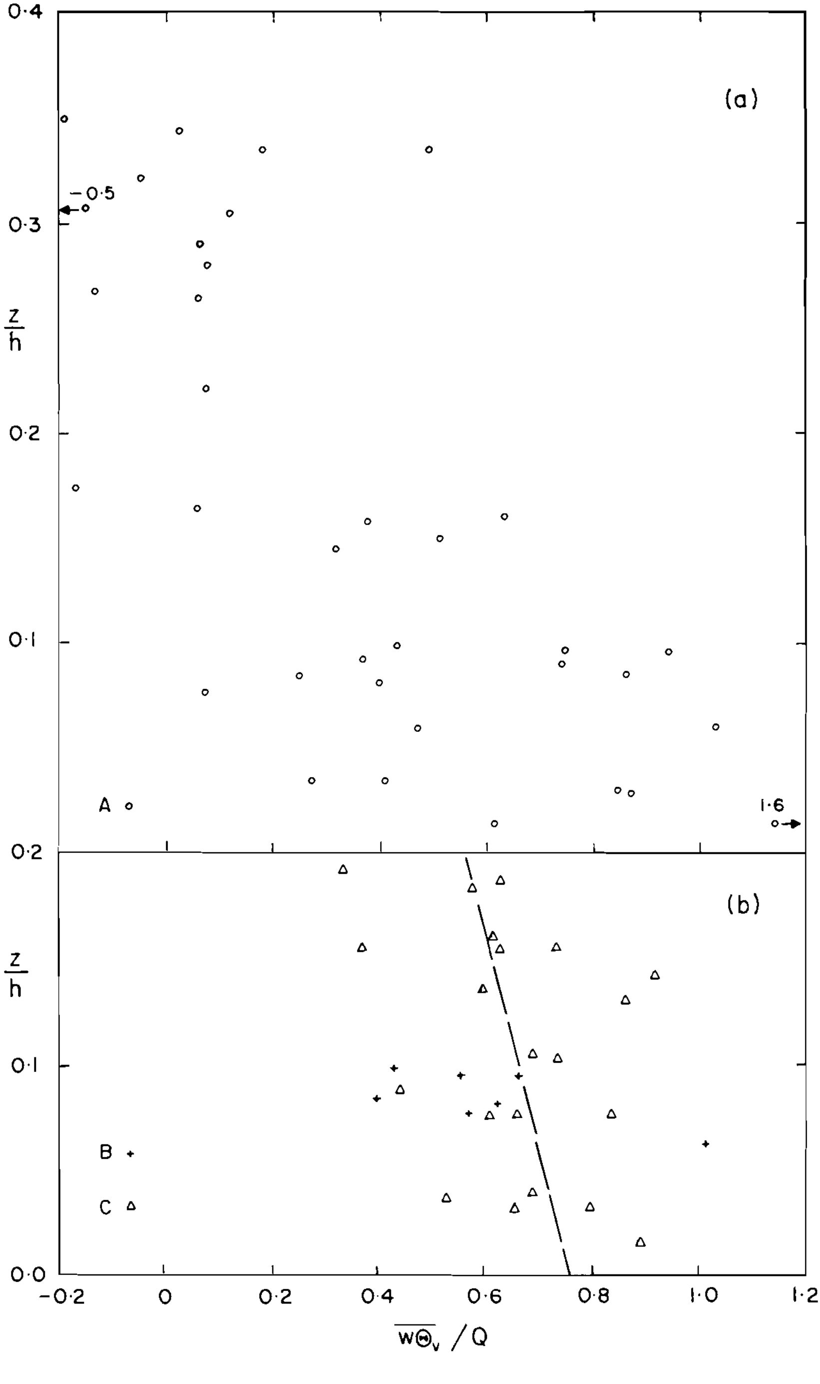

Fig. 7 Non-dimensional heat flux against the non-dimensional height, z/h for the near-neutral Group A (above) and unstable Groups B(+) and C(Δ), (below).

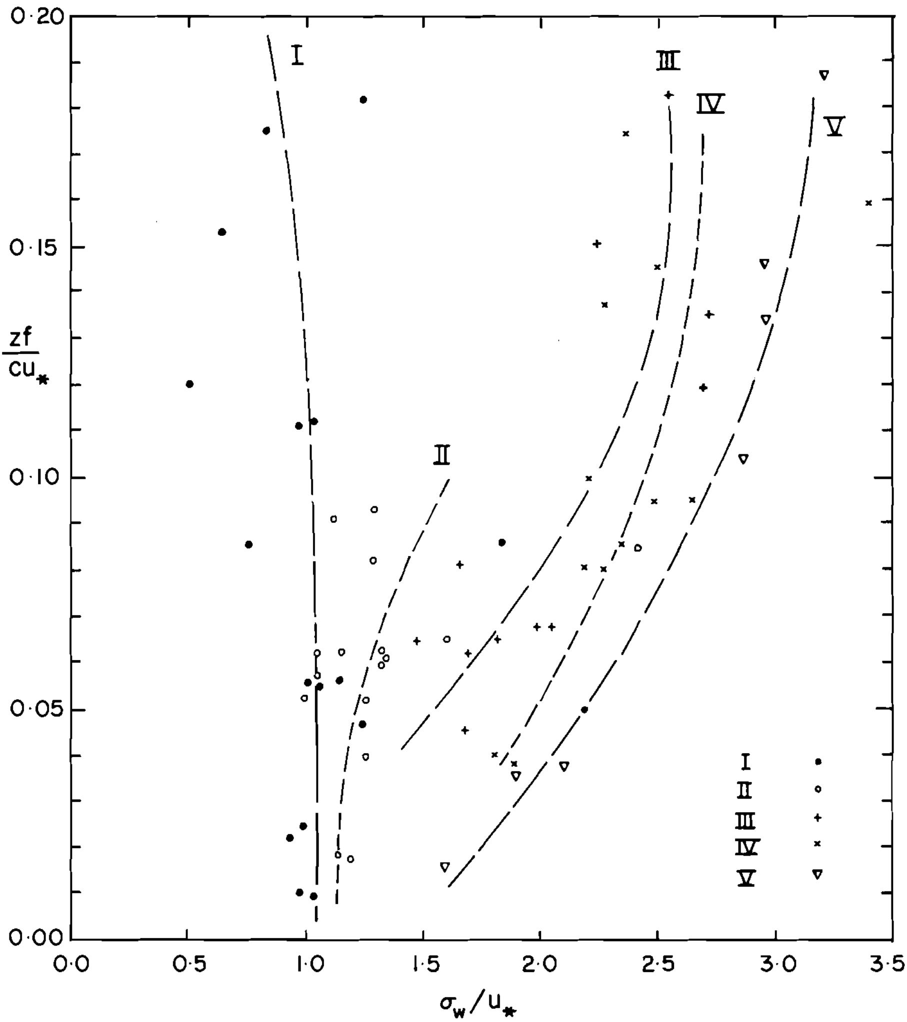

Fig. 8 Non-dimensional standard deviation of vertical velocity fluctuations against non-dimensional height, zf/cu_* ($c = 0.4$), for each stability group (I to V). The curves indicated are best fit polynomials (to order 3) to each group.

4 Practical considerations

As shown in the previous section, the best scaling parameters were h, w_* and θ_* which requires knowledge of the height to the inversion as well as the surface heat flux. An advantage of the cu_*/f, u_* and T_* scaling is that they can be specified with knowledge of the surface values only. There is no need to know the height up to the inversion. For practical reasons then the cu_*/f scaling may be more useful, particularly for those concerned with the intensity of the turbulence as a function of height.

In Fig. 8 the variations of σ_w/u_* with height and stability are demonstrated.

As shown, there is an increase of σ_w/u_* with stability at a given non-dimensional height. For near-neutral stabilities σ_w/u_* is about constant or slowly decreasing with zf/cu_* while for unstable stratifications there is a marked increase with zf/cu_*. For practical purposes one could use:

$\sigma_w/u_* \sim 1.1 - 1.6\ zf/u_*$ for near-neutral conditions, which reduces to $\sigma_w/u_* \sim 1.0$ for neutral stratifications, and $\sigma_w/u_* \sim 1.1 + 42\ zf/u_* - 300\ (zf/u_*)^2$ for unstable stratifications (the curve for Group IV). These expressions would be valid for $z < 0.1\ u_*/f \sim 10^3\ u_*$ (mid-latitudes). For over water this would be $z < 30\ \bar{u}_{10}$. Over land it will be more difficult to determine u_* from the mean wind and it is possible that the results may depend on the surface Rossby number G/fz_0 where G is the geostrophic wind speed and z_0 the roughness length.

For σ_u/u_* and σ_v/u_* the results were similar to those for σ_w/u_* but with a larger amount of scatter. For Groups I and II the curves were similar with both parameters decreasing slightly with height. The best straight line fits were:

$$\sigma_u/u_* = 2.1 - 12\,zf/u_* \qquad \sigma_v/u_* = 1.7 - 8\ zf/u_*$$

for near-neutral conditions. For the unstable Groups III, IV, and V both σ_u/u_* and σ_v/u_* increase slightly with height. The scatter is larger but straight line approximations would be valid for practical purposes. These are

$$\sigma_u/u_* = 2.3 + 6\,zf/u_* \qquad \sigma_v/u_* = 2.2 + 6\,zf/u_*$$

for unstable conditions. The comments made on σ_w/u_* apply to these results as well.

5 Summary

The turbulence in the planetary boundary layer does seem amenable to scaling by fairly simple schemes. The best of the two sets proposed in the literature seems to be to scale the heights by h, the height to the inversion, velocities by $w_* = (ghQ/T)^{1/3}$ and temperatures by $\theta_* = (Q^2T/gh)^{1/3}$, for unstable stratifications. For neutral conditions u_* may be more appropriate for velocities. The experimental results were generally in agreement with the results of the numerical models developed by Deardorff (1972) and Wyngaard et al. (1974). It is evident, however, that further experimental studies are necessary to resolve the effects of surface roughness, baroclinicity, and the lack of time stationarity.

Acknowledgments

The data were collected during IFYGL and I am grateful to those who participated in its collection and analysis. J.I. MacPherson and N. Bobbit of NAE deserve special thanks. Thanks are also due to Dr B.R. Kerman for constructive discussions of the results.

References

BROOKS, C.E.P. and N. CARRUTHERS. 1953. *Handbook of statistical methods in meteorology*. London: HMSO, 412 pp.

CLARKE, R.H. and G.D. HESS. 1973. On the appropriate scaling for velocity and temperature in the planetary boundary layer. *J. Atmos. Sci.* **30**: 1346–53.

DEARDORFF, J.W. 1972. Numerical investigation of neutral and unstable planetary boundary layers. *J. Atmos. Sci.* **29**: 91–115.

——— 1973. Three-dimensional numerical modeling of the planetary boundary layer. In *Workshop in micrometeorology*, ed. D.A. Haugen, pp. 271–311. Amer. Meteor. Soc.

——— 1973. An explanation of anomalously large Reynolds stresses within the convective planetary boundary layer. *J. Atmos. Sci.* **30**: 1070–6.

LENSCHOW, D.H. 1970. Airplane measurements of planetary boundary layer structure. *J. Appl. Meteor.* **9**: 874–84.

MCBEAN, G.A. 1971. The variations of the statistics of wind, temperature and humidity fluctuations with stability. *Boundary-Layer Meteor.* **1**: 438–57.

———, and R.D. PATERSON. 1975. Variations of the turbulent fluxes of momentum, heat and moisture over Lake Ontario. *J. Phys. Oceano.* **5**: 523–31.

———, and J.I. MACPHERSON. 1976. Turbulence above Lake Ontario. *Boundary-Layer Meteor.* (accepted for publication).

SMITH, S.D. 1973. *Thrust anemometer measurements over the sea re-examined.* Rep. BI-R-73-1, Bedford Institute of Oceanography, Dartmouth, Nova Scotia, Canada, 23 pp.

TENNEKES, H. 1973. Similarity laws and scale relations in planetary boundary layers. In *Workshop in micrometeorology*, ed. D.A. Haugen, pp. 177–216. Amer. Meteor. Soc.

WYNGAARD, J.C. 1973. On surface-layer turbulence. In *Workshop in micrometeorology*, pp. 101–49.

———; O.R. COTE; and K.S. RAO. 1974. Modeling the atmospheric boundary layer. *Adv. in Geophys.* **18A**: 193–211.

CALL FOR PAPERS – SECOND CONFERENCE ON HYDROMETEOROLOGY

The Second AMS Conference on Hydrometeorology will be held in Toronto, Canada, on 25–27 October 1977 at the Headquarters of the Atmospheric Environment Service and at the Harbour Castle Hotel. The conference will be sponsored jointly by the American Meteorological Society and the Canadian Meteorological Society with the support of the American Geophysical Union, the Canadian Society for Civil Engineering, the American Society of Civil Engineers, the Canadian Water Resources Association, and the American Water Resources Association.

The conference is designed as a forum for discussion of the hydrometeorological needs of the applied hydrologist and engineer, and as a source of information (including an audio visual display) on current techniques and data available for field use. A feature will be a panel of representatives from a cross-section of applied hydrology who will lead discussion on hydrometeorological problems facing practising hydrologists. Presentations on the techniques and resource materials currently available to practising hydrologists are also scheduled.

Other sessions, for which papers are invited, are being designed to emphasize the hydrometeorological aspects of hydrologic design and forecasting of streamflow and water supply, environmental impact, snowfall and snowmelt, and remote sensing. A general session is also planned.

Authors should submit titles and short abstracts (200 words) by 1 March 1977 to Mr H.L. Ferguson, Program Chairman, Second Conference on Hydrometeorology, Atmospheric Environment Service—ARQH, 4905 Dufferin Street, Downsview, Ontario, Canada M3H 5T4.

Instructions for the preparation of papers for the pre-printed proceedings will be furnished to those authors whose papers have been accepted. Final papers should be received no later than 1 July 1977.

The Distinction Between Canopy and Boundary-Layer Urban Heat Islands

T.R. Oke
University of British Columbia, Vancouver, B.C.

[Original manuscript received 22 March 1976; in revised form 1 June 1976]

ABSTRACT

Air temperature measurements from car traverses in and near Vancouver, B.C. are used to test two urban heat island models: one an empirical model, the other a theoretical advective model. The empirical model describes the Vancouver observations well, whereas the advective one performs rather poorly. This discrepancy may be attributed to a failure to distinguish between meteorological conditions in the urban canopy, and those in the overlying urban boundary layer. This leads to a reassessment of the explanation of the relationship between city size (as measured by population) and the heat island intensity (as measured in the urban canopy).

1 Introduction

In a previous paper (Oke, 1973) the relationship between a city's size (as measured by its population, P) and the intensity of its urban heat island, ΔT_{u-r} (as defined by the difference between the background rural and highest urban temperatures) was explored. Based on measurements from ten Québec settlements ranging in size from 1.0×10^3 to 2.0×10^6 inhabitants it was shown that ΔT_{u-r} is related to log P. With clear skies at the time of maximum heat island intensity (just after sunset, Oke and East, 1971; Hage, 1972; Oke and Maxwell, 1975), the following empirical relation was derived:

$$\Delta T_{u-r} = \frac{P^{0.27}}{4.04\bar{u}^{0.56}} \qquad (1)$$

$$\simeq \frac{P^{\frac{1}{4}}}{4\bar{u}^{\frac{1}{2}}}$$

where $\bar{u}$ is regional (10 m) wind speed (m s^{-1}) and ΔT_{u-r} is measured in °C.

Equation (1) is open to criticism because it is purely empirical in origin, and dimensionally incorrect. Summers (1964) on the other hand developed a physically-consistent theoretical model of the urban heat island based on an advective concept. The Summers model envisages stable rural air being advected across a warmer urban area. During its passage across the city the lowest layers become progressively modified due to the input of urban heat, and the increased mechanical turbulence produced by the greater urban roughness. Under certain limiting assumptions (see below) the model predicts that ΔT_{u-r} should be proportional to the square root of the distance of fetch (x) from the upwind rural/urban boundary to the city centre:

$$\Delta T_{u-r} = \left[\frac{2xQ\alpha}{\rho c_p \bar{u}}\right]^{\frac{1}{2}} \tag{2}$$

where Q is the urban surface heat output, α is the difference between the urban and rural potential temperature (θ) lapse rates, which is given by the rural value $(\Delta\theta/\Delta z)_r$ if the urban profile is assumed adiabatic (i.e. $(\Delta\theta/\Delta z)_u = 0$), ρ is the air density and c_p is the specific heat of air at constant pressure. Equation (2) is strictly valid only for the simple case of a spatially uniform heat source (Q) and a steady wind with no shear, but has been applied over a wider range of conditions.

The empirical fourth root of P result in (1) could be interpreted as being consistent with (2) from simple geometrical arguments (Ludwig, 1970; Oke, 1973). In a circular city the distance x is the radius r and is therefore proportional to the square-root of the built-up area, A ($A = \pi r^2$). In North America P is proportional to A raised to an exponent close to unity (Tobler, 1969). Hence with $\Delta T_{u-r} \propto r^{1/2}$, and $r \propto P^{1/2}$ we might expect $\Delta T_{u-r} \propto P^{1/4}$.

In the present study both of the above models are tested using data from the same city.

2 Survey area and measurement

The urban heat island and temperature lapse rate data used in this study were gathered by automobile traverses in and near Vancouver, B.C. (Fig. 1). The metropolitan region is located at the mouth of the Fraser River Valley. It is surrounded to the east and south by mixed farming and residential areas, to the west by the waters of Georgia Strait, and to the north by the Coastal Mountains which rise abruptly to a height of about 1.3 km. The total population of the urban region is approximately 1.1×10^6. The most densely settled and intensely built-up area is ex-central, being located on Burrard Peninsula (Fig. 1).

Air temperatures were monitored with a thermistor probe sensor (response time 0.8 s) and recorded on a chart recorder to a relative accuracy of ±0.2°C (Oke and Fuggle, 1972). The probe was mounted approximately at 1.5 m, and to one side away from the vehicle. The probe was shielded against radiation and aspirated at a rate of 3.5 m s^{-1}.

Data gathering involved three modes of traverse. On some occasions as many as six cars covered an area of the metropolitan region in closed traverses, each taking approximately 1.5 to 2 h. This provided a complete spatial distribution of air temperatures. On other occasions only one car was used to complete a 40 km closed traverse in approximately 1 h. The route (Fig. 1) was identical to that described in Oke and Maxwell (1975), and was chosen to provide a complete rural/urban cross-section (based on the experience gained from the spatial distribution traverses). Sometimes in conjunction with one of the above

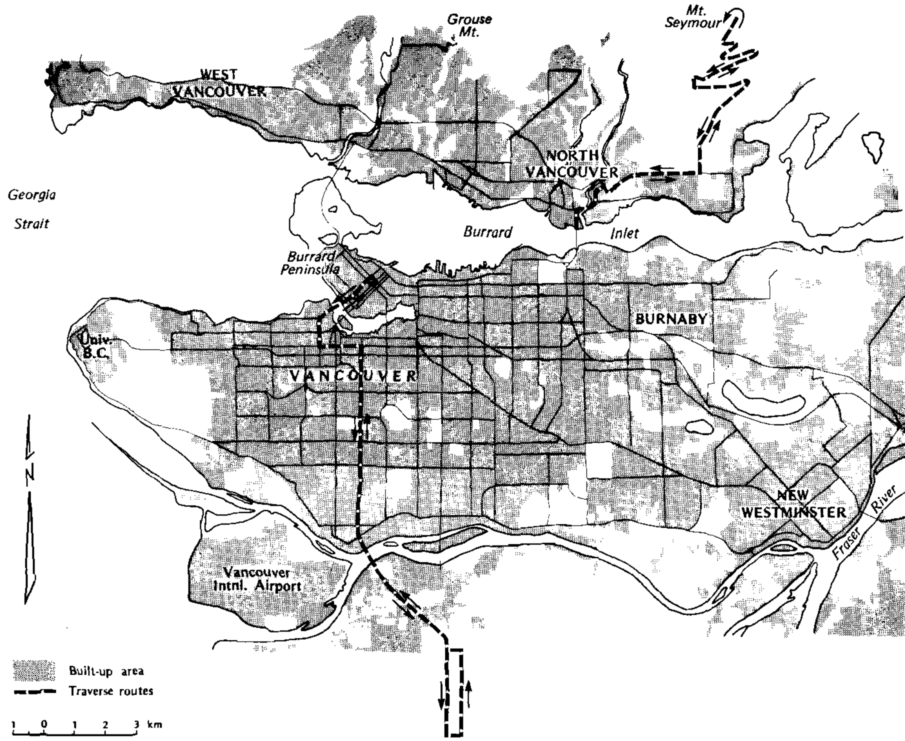

Fig. 1 Location and land use map of Vancouver, B.C., including outline of built-up areas and automobile traverse routes.

two modes a car traversed the Mt Seymour Highway (Fig. 1). This provided a temperature profile extending essentially from sea-level to an elevation just greater than 1 km. This profile was used to estimate a first approximation to the free air rural lapse rate. The lapse rate was estimated as the average slope of the temperature profile between 200 m above sea level, and any major break in the profile above. The lowest 200 m layer was omitted because of suspected urban and water body effects. Lapse rates measured in this manner have been found to compare very favourably with those from a light aircraft flying over Burrard Inlet, and from a gondola running up Grouse Mt. (Fig. 1) by Suckling et al. (1975).

Corrections were applied to the raw data to account for temperature change during the traverse period, and to make allowance for height differences. The time-based corrections were applied assuming linear temperature change with time. This appears to be approximately correct for data collected, as in this case, about 1–3 h after sunset (Oke and Maxwell, 1975). Height corrections were performed by converting the time-corrected environmental temperatures to potential temperature (θ) standardized to a pressure of 1000 mb. The change in heat island intensity due to this correction is minimal. Hence the more familiar symbolization ΔT_{u-r} is retained.

Suitable ΔT_{u-r} data to test the Oke (1973) relationship were available from 37 of the traverse nights (15 spatial surveys and 22 cross-section traverses). The data only refer to the time of near maximum heat island development (approximately 1–3 h after sunset), when skies were near cloudless ($\leqslant$2 tenths Cirrus). Data to test the Summers (1964) model were available from 26 nights (20 of the cloudless nights used above, and 6 with >2 tenths Cirrus). The smaller data set was due to the requirement of simultaneous observations of ΔT_{u-r} and vertical lapse rate. The data were gathered in the period 1972–75, and include all seasons of the year.

Hourly meteorological observations of wind speed at a height of 10 m, wind direction, cloud amount and type, and total atmospheric pressure were abstracted from the Vancouver International Airport (Fig. 1) records.

3 Model tests

a *Oke (1973)*

Fig. 2 shows the relationship between ΔT_{u-r} and $\bar{u}$ for Vancouver with cloudless skies. After transformation, linear regression analysis yields:

$$\Delta T_{u-r} = \frac{9.63}{\bar{u}^{0.52}} \tag{3}$$

with a coefficient of determination $r^2 = 0.62$, and a standard error-of-estimate for ΔT_{u-r} $(S_{\Delta T}) = \pm 1.36°C$. Comparison of the original Québec model (1) with this Vancouver relationship (Fig. 2) reveals remarkable agreement. The maximum difference between the two over the range of $\bar{u} = 1$ to 11 m s^{-1} is approximately 8% at 1 m s^{-1}. (Note that (1) was derived for $\bar{u} < 6$ m s^{-1} and hence its extrapolation to higher speeds is only tentative.)

The upper and lower limits of a relation such as (3) do provide some difficulties in estimating such interesting features as the maximum heat island intensity ($\Delta T_{u-r(\max)}$), and the critical wind speed at which the heat island is obliterated $\bar{u}_{\text{crit}}$. As winds drop below 1 m s^{-1} the form of (3) will increasingly tend to overestimate ΔT_{u-r} because it ignores the fact that there are limits to the intensity (Oke, 1973). These limits include the generation of thermal breezes, which tend to diminish urban/rural contrasts, and the finite availability of energy. Equally the data precision decreases at small $\bar{u}$ because of instrument limitations and the spatial complexity of the wind field. As a consequence of these problems it is not possible to extrapolate (3) to find $\Delta T_{u-r(\max)}$. The maximum spot value measured was 11.6°C (see Fig. 4). This is slightly larger than originally reported by Oke (1973) and modifies the relation derived therein relating $\Delta T_{u-r(\max)}$ to P for 18 North American cities:

$$\Delta T_{u-r(\max)} = 2.96 \log P - 6.41.$$

The new relation is:

$$\Delta T_{u-r(\max)} = 3.06 \log \mathrm{P} - 6.79$$

and gives improved statistics of $r^2 = 0.97$ and $S_{\Delta T} = \pm 0.6°C$.

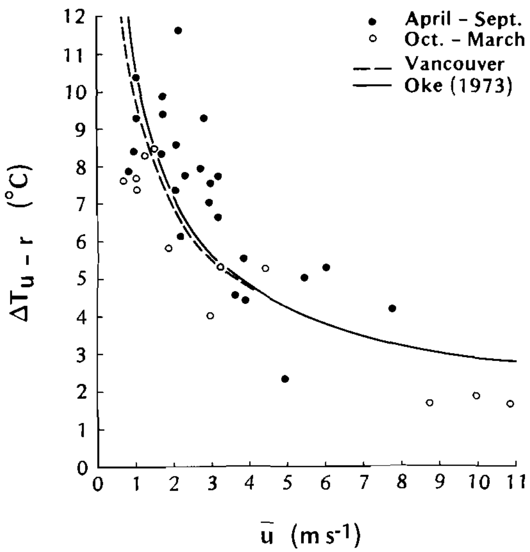

Fig. 2 Relation between measured heat island intensity and regional wind speed for Vancouver, B.C. Data gathered at about 1–3 h after sunset on cloudless nights. Dashed line is least squares regression fit to the Vancouver data, and the solid line is from Oke (1973) based on 10 Québec settlements.

On the other hand the value of $\bar{u}_{crit}$ for Vancouver is difficult to assess due to the sparseness of the data beyond $\bar{u} = 6$ m s^{-1} (Fig. 2). Oke and Hannell (1970) developed an equation for $\bar{u}_{crit}$ from log P. For Vancouver this suggests $\bar{u}_{crit}$ should be approximately 9 m s^{-1}, but according to Fig. 2 this appears to be an underestimate. This may be due to the use of standard climatological and not traverse data in constructing the original equation. The former tend to underestimate ΔT_{u-r} because the stations are often located in parks, and only by chance are they located in the heat island core. The inclusion of cloudy sky data would operate in the same direction.

There is evidence of a seasonal bias in Fig. 2 with a tendency towards a relatively larger heat island for a given wind speed in the warmer half of the year. It is not appropriate to speculate as to the physical cause of such an effect. It should be noted, however, that the absolute magnitude, and the seasonal variation of anthropogenic heat output Q_F from Vancouver is not large. Yap (1973) calculated the winter flux density for Vancouver City to be 23 W m^{-2}, and for the summer 15 W m^{-2}. Probably more important to the heat island is the strong contrast in seasonal climate characteristics (e.g. air mass stability, moisture availability, solar absorption, etc.).

Despite some small problems, we may reasonably conclude that the Vancouver results provide support for the simple model of Oke (1973). This is important because an empirical model such as this requires verification with an independent data set.

b *Summers (1964)*

Equation (2) was evaluated for each case assuming that x represented the distance between the upwind urban/rural boundary and the core of the heat island. This gave a range of fetches from $x = 0.5$ km with winds from the NNE, to 17 km with winds from ESE.

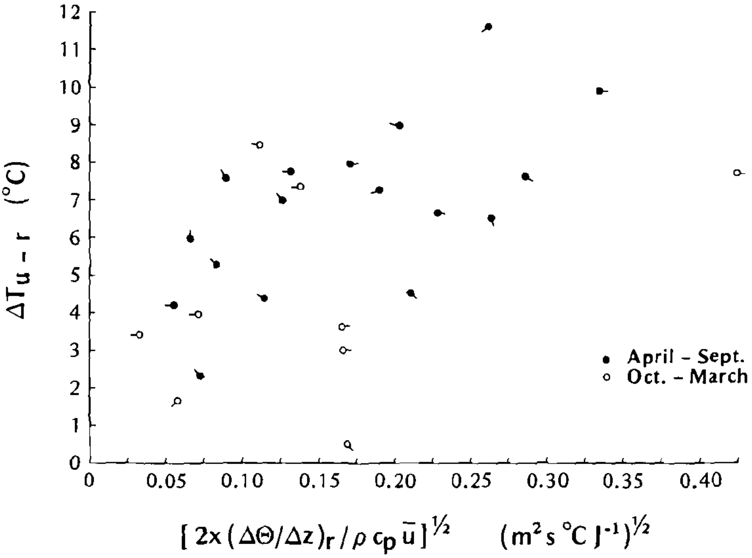

Fig. 3 Relation between measured heat island intensity and the Summers (1964) advective model calculations. The "arrows" on each point represent the wind direction based on a 360° compass.

The relationship between ΔT_{u-r} and the product $[2x(\Delta\theta/\Delta z)_r/\rho c_p \bar{u}]^{1/2}$ is given in Fig. 3. The result is not very satisfactory for three main reasons. Firstly, the scatter of points is rather large. Linear regression produced rather weak statistics with $r^2 = 0.27$, and $S_{\Delta T} = \pm 2.32$°C. Secondly it follows from (2) that the slope of this relationship should be $Q^{1/2}$ and on this basis the average value of $Q = 208 \pm 24$ W m^{-2}. This is approximately one order of magnitude larger than the Vancouver Q_F values mentioned earlier, and substantially larger than the turbulent sensible heat fluxes measured in Vancouver at this time of night both above roof level (Yap and Oke, 1974), and within canyon (Nunez and Oke, 1976). In addition there appears to be no obvious seasonal variation in Q. Thirdly the scatter in Fig. 3 appears to depend on the direction of fetch (as indicated by the "arrows" in each case), and surprisingly the relatively large ΔT_{u-r} values at each given value on the abscissa (i.e. implying relatively large Q) are associated with the shortest fetches from the W and N quadrants, and the smallest values with long urban trajectories from the E and S (Fig. 1). A particularly striking example of this is exhibited by the heat island map for 4 July 1972 (Fig. 4), when $\Delta T_{u-r(\max)}$ was recorded. The observation period

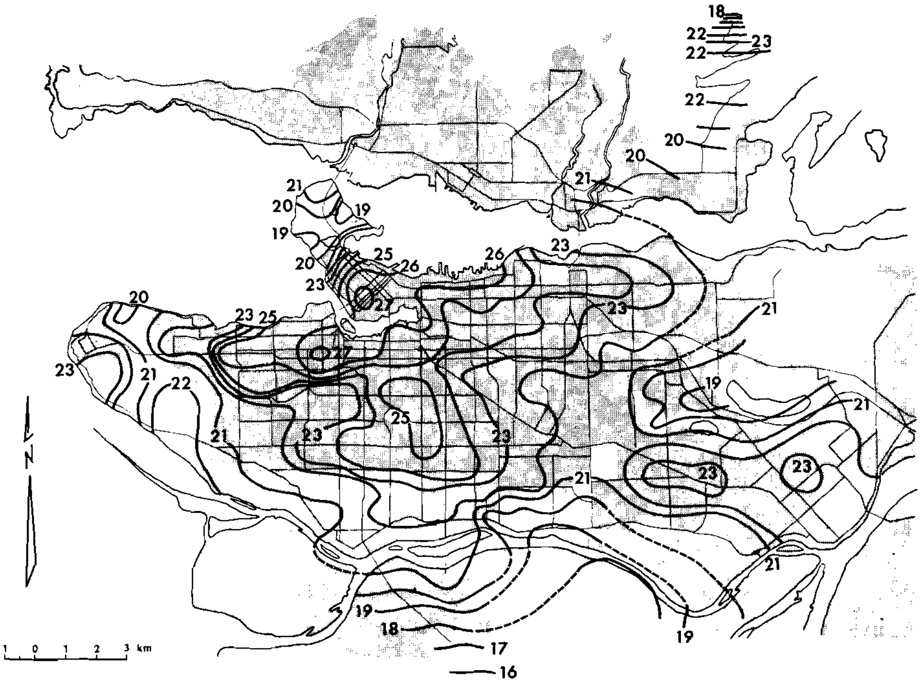

Fig. 4 Two-dimensional temperature distribution in Vancouver, B.C. at 2100 PST on 4 July 1972 with clear skies, and with winds W and NW at 2.0 m s^{-1}. Isotherms are time-corrected potential temperatures (°C).

was characterized by W and NW airflow off the water (surface temperature 20°C), giving a very short urban fetch (< 2 km) to the heat island core. Such a situation is antithetic to the Summers cumulative heat advection mechanism.

The above is not a thoroughly rigorous test of the Summers model, for example in the use of 10 m wind data instead of that for the whole mixing layer; and the use of mountainside traverses to approximate the free air sounding. However, most errors attributable to these approximations will only cast doubt on the absolute values and not upon the generally weak form of the relationship, and could do nothing to alleviate the problem associated with the "inverse-fetch" effect.

4 Discussion

It is hypothesized here that there are at least two different heat islands produced by urbanization. The proposed classification which follows recognizes two layers of the atmosphere: one is governed by processes acting at the microscale; the other by those at the local or mesoscale.

The first layer may be termed the *urban canopy* (Fig. 5), consisting of the air contained between the urban roughness elements (mainly buildings). The urban canopy is a microscale concept, its climate being dominated by the nature of the immediate surroundings (especially site materials and geometry). The

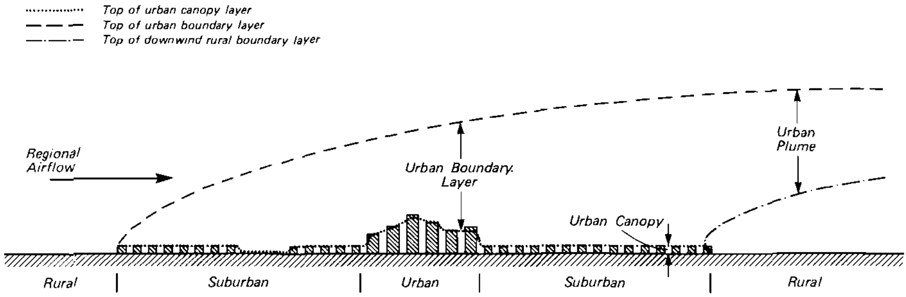

Fig. 5 Schematic representation of the urban atmosphere illustrating a two-layer classification of thermal modification.

upper boundary of the urban canopy is likely to be imprecise because of the nature of the urban "surface" (c.f. vegetative canopies). In densely built-up areas the limit is visualized to lie at, or just below, roof level; in large open spaces it may be entirely absent. The depth of this layer may also be a function of wind speed, shrinking as stronger airflow allows influences from above to penetrate.

The second layer, situated directly above the first may be called the *urban boundary layer* (Fig. 5). This is a local or mesoscale concept referring to that portion of the planetary boundary layer whose characteristics are affected by the presence of an urban area at its lower boundary. The modified layer is conceived to develop as an advective internal boundary layer. In the downwind region this layer may become separated from the surface as a new rural boundary layer develops underneath, and this has been termed the *urban plume* (Clarke, 1969). The top of the urban boundary layer is commonly capped by a temperature inversion giving some correspondence with the upper limit of urban pollution.

The evidence to support this conceptual hypothesis is neither direct nor complete at this time, but the problems experienced here with the Summers approach could be viewed as an inappropriate mixture of heat island measurements in the *canopy layer*, with a model based on *boundary-layer* mechanisms. If so, the same error was incurred by Summers (1964) when he tested his model using surface minima data from climatological stations. The approximate agreement obtained may have been fortuitous since both his estimates of ΔT_{u-r}, and Q (see Leahey and Friend, 1971) were too low. Evidence of the inappropriateness of this advective approach to explain canopy measurements of ΔT_{u-r} is provided in this study by replacing the variable fetch in (2) by a constant value of x. This is the primary operator in the advective approach and its removal should decrease the predictive power of the relation. On the contrary, however, its absence actually improves the fit compared to that in Fig. 3, giving $r^2 = 0.57$ and $S_{\Delta T} = \pm 1.78°C$. This strongly suggests that urban fetch is not important in explaining canyon measurements of ΔT_{u-r}.

Relegating the role of advection in the formation of the canopy heat island would seem to largely negate the explanation for the fourth root of P relationship given in section 1. It now seems reasonable to suggest that P may be less a surrogate for *distance* and more one for the *physical structure* of urban central areas. This would mean that cities with a greater number of inhabitants exhibit more extreme signs of urbanization in their core areas and therefore greater thermal modification. For example, as a city's population grows the size of the buildings in the core increases; the sky view factors for long-wave radiative cooling decrease; the heat capacity of the construction materials and the thermal inertia of the structures increase; the density of anthropogenic heat emission increases; the amount of vegetation decreases, etc. Such an explanation appears reasonable, but in the absence of more direct measures cannot be verified.

Unwin and Brown (1975) provide indirect support when they note an almost perfect linear relationship between the proportion of city area modified (i.e. unnatural) and log P using data from cities in the United States compiled by Marotz and Coiner (1973). Their modification term represents the whole city and not just the core area, but it may be assumed to be indicative of the urbanization process. If this hypothesis is correct, then the differing slopes relating $\Delta T_{u-r(\max)}$ to log P found for North American and European settlements (Oke, 1973) may be explainable in terms of the different urban morphologies of city centres in the two regions. It is a general observation that North American city core areas exhibit more tall buildings than is the case in Europe.

The hypothesis that P is a surrogate for physical structure rather than distance of fetch would also explain the results of Chandler (1967). In a study of the heat islands of Leicester ($P = 0.27 \times 10^6$, $A = 70$ km^2) and London ($P = 8.25 \times 10^6$, $A = 1940$ km^2) it was shown that despite their disparity in size (and therefore fetch), the urban/rural temperature differences were closely comparable if comparison was made between areas of "similar housing density" in the two cities. These results were previously considered to be inexplicable by Oke (1973) in the context of his model.

5 Conclusions

The study shows that a simple empirical model incorporating city size and wind speed is better able to describe urban heat island observations from car temperature traverses than a physical model based on an advective concept. The relatively poor performance of the advective model highlights the need to separate the climate of the urban canopy (the air beneath roof level) from that of the urban boundary layer above. It would appear that the canopy thermal climate is governed by the immediate site character (especially building geometry and materials), and not by the accumulation of thermally modified air from upwind areas. If there are two distinct layers and heat islands, governed by different process ensembles – this will require different theoretical frameworks for modelling and different observation platforms and networks for their description. Similarly it will be very important to study the extent to which these layers are coupled.

Acknowledgments
This work was conducted under grants made available from the National Research Council of Canada and Environment Canada (Atmospheric Environment Service). Thanks are also due to K. Nicol and E. Sumpton who assisted during some of the automobile traverses, and to the Vancouver International Airport Weather Office which supplied forecast and climatological information. The figures were drawn by P. Jance.

References

CHANDLER, T.J. 1967. Night-time temperatures in relation to Leicester's urban form. *Meteor. Mag.* **96**: 244–50.

CLARKE, J.F. 1969. Nocturnal urban boundary layer over Cincinnati, Ohio. *Mon. Wea. Rev.* **97**: 582–9.

HAGE, K.D. 1972. Nocturnal temperatures in Edmonton, Alberta. *J. Appl. Meteor.* **11**: 123–9.

LEAHEY, D.M. and J.P. FRIEND. 1971. A model for predicting depth of the mixing layer over an urban heat island with applications to New York City. *J. Appl. Meteor.* **10**: 1162–73.

LUDWIG, F.L. 1970. Urban air temperatures and their relation to extra urban meteorological measurements. *Amer. Soc. Heat. Refrig. Air-Cond. Engin.* Publ. No. SF-70-9, 40–5.

MAROTZ, G.A. and J.C. COINER. 1973. Acquisition and characterization of surface material data for urban climatological studies. *J. Appl. Meteor.* **12**: 919–23.

NUNEZ, M. and T.R. OKE. 1976. Long-wave radiative flux divergence and nocturnal cooling of the urban atmosphere. **II** Within a canyon. *Boundary-Layer Meteor.* (in press).

OKE, T.R. 1973. City size and the urban heat island. *Atmos. Environ.* **7**: 769–79.

———, and C. EAST. 1971. The urban boundary layer in Montréal. *Boundary-Layer Meteor.* **1**: 411–37.

———, and R.F. FUGGLE. 1972. Comparison of urban/rural counter and net radiation at night. *Boundary-Layer Meteor.* **2**: 290–308.

———, and F.G. HANNELL. 1970. The form of the urban heat island in Hamilton, Canada. *WMO Tech. Note* No. 108: 113–26. Geneva: World Meteor. Org.

———, and G.B. MAXWELL. 1975. Urban heat island dynamics in Montréal and Vancouver. *Atmos. Environ.* **9**: 191–200.

SUCKLING, P.W.; R. HARDY; K. LOVE; and W. TANNER. 1975. Preliminary results on the vertical temperature structure of Vancouver. Paper presented to 9th Annual Congress Canadian Meteorological Society, Vancouver, B.C., 8 pp.

SUMMERS, P.W. 1964. An urban ventilation model applied to Montréal. Unpub. Ph.D. thesis, McGill University, Montréal.

TOBLER, W.R. 1969. Satellite confirmation of settlement size coefficients. *Area* **1**: 30–4.

UNWIN, D.J. and V.J. BROWN. 1975. Land-use and the urban heat island. Paper presented at meeting of Assn Brit. Climatol., Manchester, U.K., 7 pp.

YAP, D.H. 1973. Sensible heat fluxes measured in and near Vancouver. Unpub. Ph.D. thesis, University of British Columbia, Vancouver, 174 pp.

———, and T.R. OKE. 1974. Sensible heat fluxes over an urban area – Vancouver, B.C. *J. Appl. Meteor.* **13**: 880–90.

A Revised Method for Determining the Direct and Diffuse Components of the Total Short-wave Radiation

John E. Hay
Department of Geography, University of British Columbia, Vancouver

[Manuscript received 25 May 1976; in revised form 10 August 1976]

ABSTRACT

A relationship, derived by Liu and Jordan (1960), under which the total short-wave radiation may readily be subdivided into its direct and diffuse components is shown to vary both spatially and seasonally. This variability is attributed to changes in the importance of the multiple reflection of short-wave radiation between the earth's surface and atmosphere. A revised relationship, which incorporates the influence of this process, is shown to have applicability at a large number of Canadian locations.

1 Introduction

Increased utilization of solar energy in the 1970s has resulted in greater interest in the amount of short-wave radiation (wavelengths $<4.0\ \mu m$) incident upon a surface of given orientation, as specified by its tilt and aspect. However, the more readily available observational data are characteristically for the more restricted, and commonly less appropriate, horizontal surface. Kondratyev (1969) and others have presented methods for calculating the radiation on a non-horizontal surface given the energy incident on a horizontal surface, but the approach requires a knowledge of the proportions of the total short-wave radiation ($K\downarrow$) reaching the surface as direct ($S\downarrow$) and diffuse ($D\downarrow$) short-wave radiation. These components are routinely measured at only a few locations in comparison to the more widespread measurements of the total short-wave radiation, but analyses of some of the available data have shown that a relationship between the short-wave radiation and its component fluxes does exist (e.g. Liu and Jordan, 1960). More complex calculation methods have been evaluated (e.g. Sadler, 1975), but the simplicity of the Liu and Jordan approach has led to its widespread adoption (e.g. Hunn et al., 1975; Löf and Tybout, 1973).

However, the Liu and Jordan model was derived from data for only one location (Blue Hill, Massachusetts) and has had little independent testing. Ruth and Chant (1976) tested the relationship using available data for four Canadian locations and found that the Liu and Jordan approach generally underestimated the ratio of $D\downarrow$ to $K\downarrow$ for a given ratio of $K\downarrow$ to K_0 (the extra-terrestrial short-wave radiation). They attributed the discrepancy to a latitude dependence in the relationship, though the physical factors involved were not

TABLE 1. Canadian stations with regular measurements of diffuse and total short-wave radiation

	Latitude (N) ° ′	Longitude (W) ° ′	Record Used
Toronto Met. Res. Stn	43 48	79 33	1967–1975
Toronto Scarborough	43 43	79 14	1960–1967
Montreal Jean Brébeuf	45 30	73 37	1965–1974
Goose Bay	53 18	60 27	1962–1975
Resolute	74 43	94 59	1960–1974

discussed. It is the purpose of this paper to evaluate the performance of the Liu and Jordan model at selected Canadian locations, to provide reasons for its demonstrated inapplicability, and to describe and substantiate the validity of a revised method for determining the component fluxes of the total short-wave radiation.

Observational data from five locations in Canada are available to investigate the relationship between the total short-wave radiation and its direct and diffuse components. The data are collected and published by the Canadian Atmospheric Environment Service. Table 1 provides details of the data record used in the present study. A departure from the computational procedures used by Liu and Jordan is that this study uses mean hourly rather than mean daily values for each month. The benefit of presenting averages for a shorter time interval is that the values of $S\downarrow$ and $D\downarrow$ determined from the relationship are commonly used as input to equations with a validity for hourly, or even shorter, time periods. The alternative is to determine daily values of $S\downarrow$ and $D\downarrow$ and then to estimate hourly values from the daily totals (Duffie and Beckman, 1974). The current wider availability of hourly values increases the desirability of working directly at the more appropriate time scale (rather than deriving them by a much more devious method).

2 Evaluation of the Liu and Jordan approach

Fig. 1 presents the data for four Canadian locations in a format similar to that used by Liu and Jordan in their analysis of the Blue Hill data. Due to the unreliability at low radiative fluxes of both the measured values and, to a greater extent, the ratios they determine, data have not been plotted when $K\downarrow$ was less than 42 $kJm^{-2}h^{-1}$. The value for K_0 was based on a solar constant of 1354 W m^{-2} and calculated as a mean hourly value for each day of each month and subsequently averaged to provide monthly mean values for each hour. Since Liu and Jordan used a value of 1396 W m^{-2} and did not average the K_0 values in the same manner, there is an opportunity for slight discrepancies between the results of the two analyses.

The Liu and Jordan type relationship is not particularly well followed at the Canadian locations, judging by the amount of scatter for each of the stations and particularly for Resolute. Moreover, ignoring for the moment the scatter for individual stations, the general relationship is not consistent between

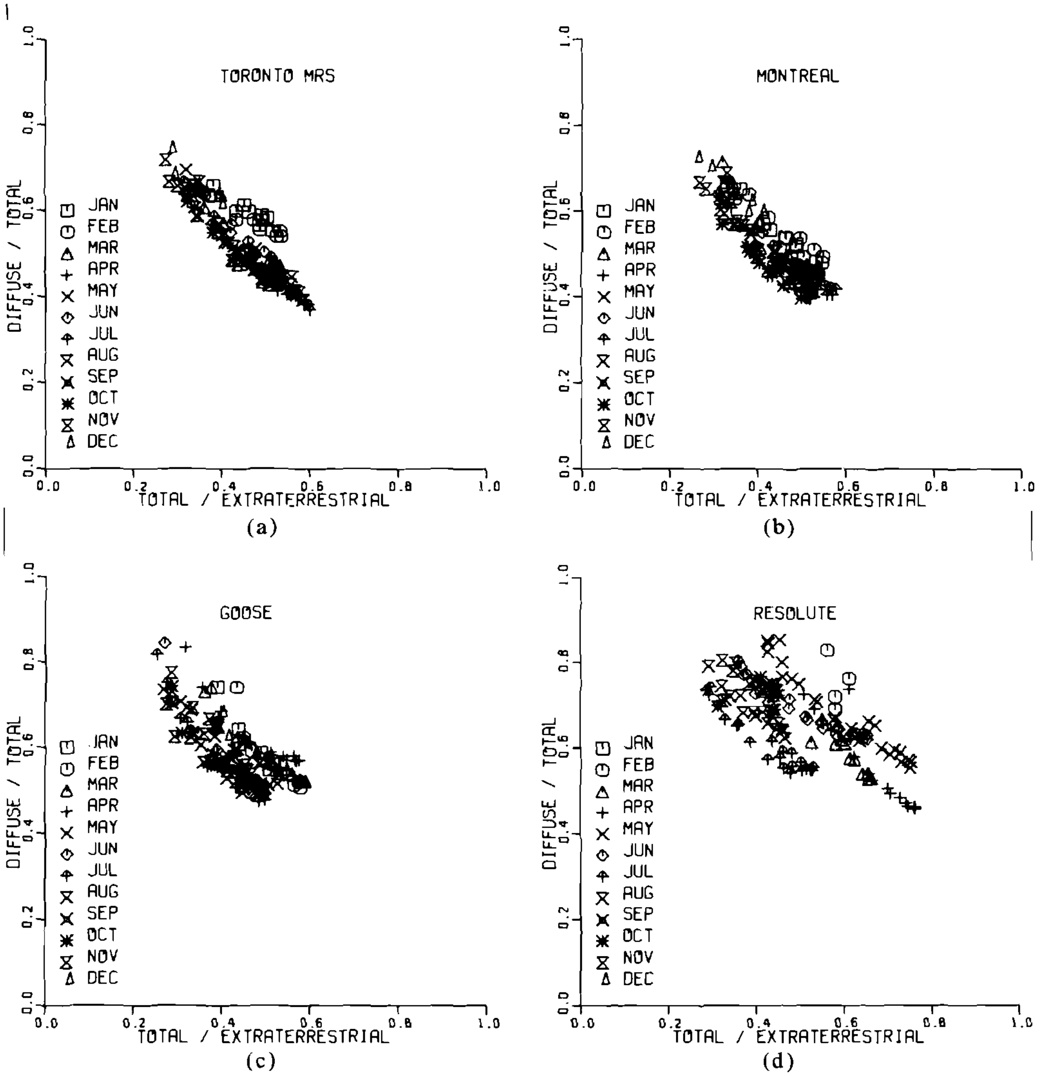

Fig. 1 Relationship between the ratios of mean hourly values of diffuse to total short-wave radiation at the surface, and of mean hourly values of the total to extra-terrestrial short-wave radiation for (a) Toronto Meteorological Research Station; (b) Montreal Jean Brébeuf; (c) Goose Bay; (d) Resolute

stations. Part of the scatter for individual station data is undoubtedly due to the use of several mean hourly values rather than a single mean daily value for each month, but this is by no means a complete explanation. Resolute (Fig. 1d) is a particularly good example of the nature of the scatter. For any given month a reasonably well-developed relationship exists with the slope being similar from month to month. The overall scatter in the Resolute data is a consequence of a seasonal variation in the constant term (intercept value) in the equation of a straight line representing the relationship for any given month. Highest values occur in the winter months and lowest in the summer months.

This same general pattern appears to hold if one makes a station-to-station comparison, as opposed to a month-to-month comparison for any single station. In this case the tendency is for the intercept value to vary with the latitude of the location. In addition, for any one lower latitude station, the seasonal variation (and hence the scatter) appears to decrease. These two trends can be extended by introducing the relationship derived by Liu and Jordan (1960) for an even lower latitude location, that of Blue Hill (42°13′N). Over the range of ratios being examined here the Blue Hill relationship is approximately linear with a similar slope but an apparent intercept value which is even lower than those of the southern Canadian stations. It is not pertinent to discuss here the relative amount of scatter in the Blue Hill relationship since, as noted earlier there is a difference in the way the data have been averaged. However, the relationship between scatter and latitude implied by the Canadian data alone would tend not to support Liu and Jordan's use of a single line to represent the relationship between the two ratios.

Despite the obvious validity of the Liu and Jordan approach for the Blue Hill data, it is now apparent that such a relationship is inappropriate for Canadian locations. Not only does the relationship undergo spatial variability but also seasonal variability for a given location. The following sections will attempt to determine the cause of this variability and develop a relationship which overcomes the limitations of the Liu and Jordan approach.

3 The influence of multiple reflection

This paper advances the hypothesis that the apparent latitudinal and obvious seasonal variations in the Liu and Jordan relationship are primarily a result of multiple reflection of short-wave radiation between the earth's surface and the overlying atmosphere. The multiply-reflected component has been shown to be an important, though far from dominant, fraction of the total incoming short-wave radiation, especially under conditions of high surface albedo or reflectivity (Hay, 1970; Sawchuck, 1974; Catchpole and Moodie, 1971). The process of multiple reflection is a result of diffuse scattering and it will increase the total incoming short-wave radiation largely as a result of an increase in the diffuse component. Both the ratio expressing the transmission of the atmosphere to the total short-wave radiation and the ratio of diffuse to total short-wave radiation will increase with multiple reflection, though the Liu and Jordan relationship implies that these two ratios are inversely related. The effect of multiple reflection is to displace data points in Fig. 1 further upwards and to the right of the origin compared to their position if multiple reflection were not occurring.

Multiple reflection is a function of both the surface albedo and the atmospheric "back-scatterance" (Möller, 1965). The size of the spatial and temporal variabilities in the former parameter can be seen from the data presented in Table 2. These are "regional" albedos rather than "site" albedos since the

TABLE 2. Monthly mean values of surface (α) and cloud base (α_c) albedos used in study. Source: Hay, 1970

		Jan	Feb	Mar	Apr	May	Jun	Jul	Aug	Sep	Oct	Nov	Dec
Toronto	α	50	50	38	28	25	25	25	25	25	25	29	39
Met. Res.	α_c	58	56	53	51	50	48	49	50	53	53	56	57
Toronto	α	50	50	38	28	25	25	25	25	25	25	29	39
Scarborough	α_c	58	56	53	51	50	48	49	50	53	53	56	57
Montreal	α	32	33	25	22	20	20	20	20	20	20	23	28
Jean Brébeuf	α_c	57	55	53	52	50	50	50	50	52	54	57	56
Goose Bay	α	55	56	50	50	35	25	25	25	25	30	35	52
	α_c	56	55	54	56	52	52	53	54	54	57	57	53
Resolute	α	80	80	79	76	69	45	26	21	45	59	74	79
	α_c	57	52	49	45	52	49	51	54	60	60	56	58

multiple reflection process involves surfaces some distance away from the radiation instrument site. Considering the influence of albedo alone, Table 2 indicates that for those stations both the overall relative importance and the intra-annual variability of multiple reflection will be greatest at Resolute.

It appears that variability in the extent of multiple reflection may explain why the Blue Hill relationship is not generally applicable and why the spatial and temporal variabilities in the Liu and Jordan relationship are as described earlier. The following section attempts to reduce these variabilities and increase the specificity of the relationship by at least semi-empirically incorporating the effect of multiple reflection.

4 Modification of the Liu and Jordan approach

A possible modification to the Liu and Jordan approach is to express the relevant ratios in terms of the short-wave radiation fluxes before multiple reflection. For the approach to be useful, these fluxes must themselves be expressed in terms of the observed radiation fluxes which include the effects of multiple reflection. The multiple reflection process is a function of the incoming radiation before multiple reflection occurs ($K{\downarrow}'$), the surface albedo (α) and the atmospheric "back-scatterance" (d) such that:

$$K{\downarrow} = K{\downarrow}' + K{\downarrow}'\,\alpha d + K{\downarrow}'\,\alpha^2 d^2 + \ldots. + K{\downarrow}'\,\alpha^n d^n + \ldots. \tag{1a}$$

$$= K{\downarrow}'/(1-\alpha d). \tag{1b}$$

Thus $$K{\downarrow}' = K{\downarrow}\,(1-\alpha d) \tag{1c}$$

If it is assumed that all the multiply-reflected radiation is diffuse

then $$D{\downarrow} = D{\downarrow}' + K{\downarrow}\alpha d \tag{2}$$

and $$D{\downarrow}' = D{\downarrow} - K{\downarrow}\alpha d \tag{3}$$

where $D{\downarrow}'$ is the diffuse short-wave radiation before multiple reflection. The two ratios now become:

$$\frac{K{\downarrow}'}{K_0} = \frac{K{\downarrow}(1-\alpha d)}{K_0} \tag{4}$$

and

$$\frac{D\downarrow'}{K\downarrow'} = \frac{D\downarrow - K\downarrow\alpha d}{K\downarrow(1 - \alpha d)} \,. \tag{5}$$

The atmospheric back-scatterance (d) may be expressed in terms of the back-scatterance for clear sky (β_0) and the cloud base albedo (α_c), weighted by the proportion of the sky hemisphere which is clear ($1 - n$) and covered by cloud (n), respectively; i.e.,

$$d = n\alpha_c + (1 - n)\beta_0. \tag{6}$$

This modified approach (using the ratios $K\downarrow'/K_0$ and $D\downarrow'/K\downarrow'$ rather than the ratios $K\downarrow/K_0$ and $D\downarrow/K\downarrow$) has been evaluated with the same data as were used in preparation of Fig. 1. Following the results of Möller (1965) β_0 was taken as 0.25. Initially the cloud base albedo was assumed equal to the cloud top albedo enabling the values of the latter parameter as calculated by Hay (1970) to be used in this study. The values used are listed along with the surface "regional" albedo values in Table 2. However, subsequent analyses using a fixed value of cloud base albedo of 0.60 (Davies et al., 1975; London, 1957; Möller, 1965) showed that the calculated values of cloud base albedo did not improve the relationship between the ratios. In fact, in cases where there was some doubt about the validity of the calculated cloud albedos (as in the case of Toronto Scarborough where cloud data for Toronto Malton had to be used), the relationship improved with the use of a constant value of 0.60 for α_c.

It is acknowledged that no attempt has been made to standardize the input data as to the period of record. While the amount of averaging involved will tend to minimize this error it is recognized that the use of unweighted and non-standardized averages will likely account for some of the scatter in the relationships being investigated. This has been accepted as a cost incurred as a result of using published data.

Fig. 2 shows the relationship between $K\downarrow'/K_0$ and $D\downarrow'/K\downarrow'$ for four Canadian stations. As a result of excluding the effect of multiple reflection, both the variability at a single station and the discrepancies between stations have been reduced. Some variability in the relationship does still exist; while part of this may be attributable to the limitations of the data, as noted above, the influence of yet other unaccounted factors cannot be ruled out. Nevertheless consideration of the effect of multiple reflection has obviously resulted in the removal of the largest portion of the variability.

On the basis of the above results, a composite relationship was determined by eye and is presented in Fig. 3. In extrapolating the relationship beyond the limits studied in the previous analysis, the general form of the Liu and Jordan (1960) relationship was maintained since they argued that there is a physical basis for the form of the relationship near its limits; the modifications developed here do not negate these fundamental controls.

The relationship as derived here is based on data from a restricted number of stations and its general spatial applicability requires further independent

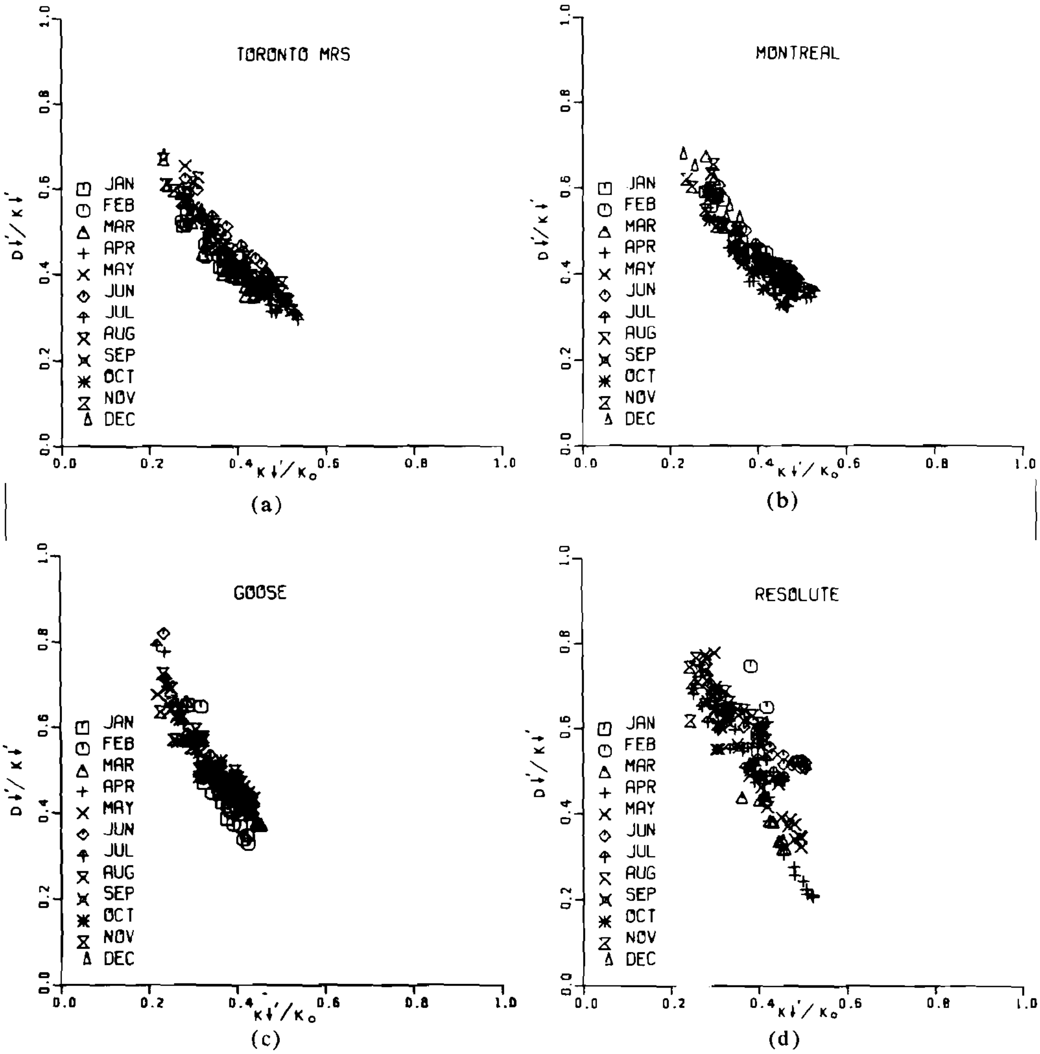

Fig. 2 Relationship between the ratios of mean hourly values of the diffuse to total short-wave radiation at the surface, and of mean hourly values of the total to extra-terrestrial short-wave radiation (excluding the multiply-reflected components of the surface fluxes) for (a) Toronto Meteorological Research Station; (b) Montreal Jean Brébeuf; (c) Goose Bay; (d) Resolute.

verification. The necessary radiation data are not routinely observed at locations other than the four stations already considered and at Toronto Scarborough. Fig. 4 provides a comparison between the observed diffuse radiation at Toronto Scarborough and that calculated using the relationship presented in Fig. 3, a value of 0.60 for α_c, and the relevant "regional" albedos listed in Table 2, and cloud cover data for Toronto International Airport Malton (Atmospheric Environment Service, 1968). The results confirm the validity

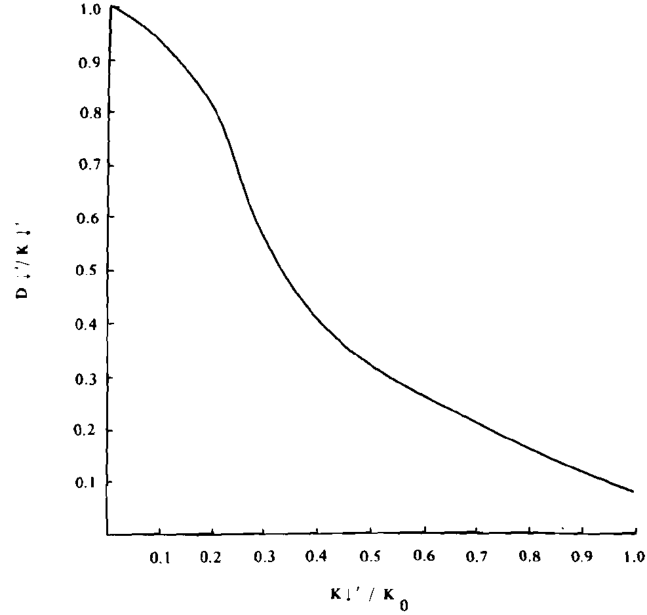

Fig. 3 The general relationship between the ratios of the mean hourly values of the diffuse to total short-wave radiation at the surface, and of mean hourly values of the total to extraterrestrial short-wave radiation (excluding the multiply reflected components of the surface fluxes).

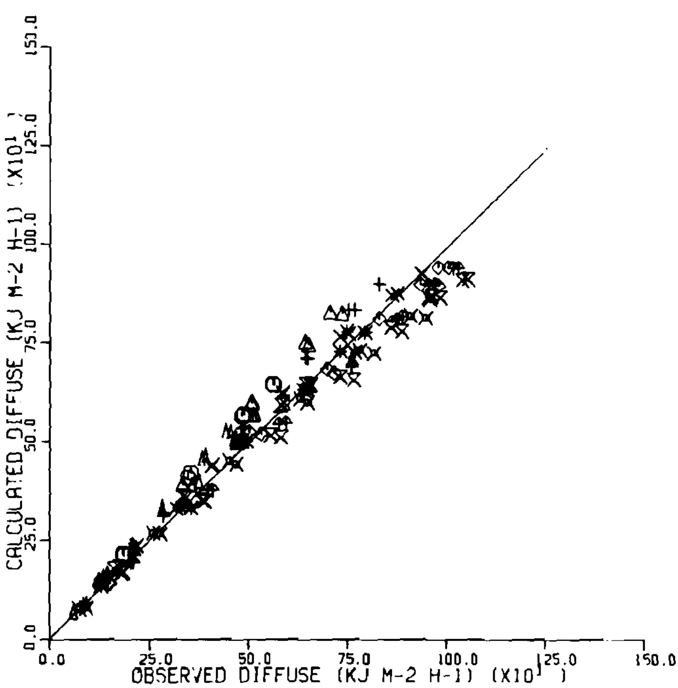

Fig. 4 Comparison of observed and calculated diffuse short-wave radiation for Toronto Scarborough.

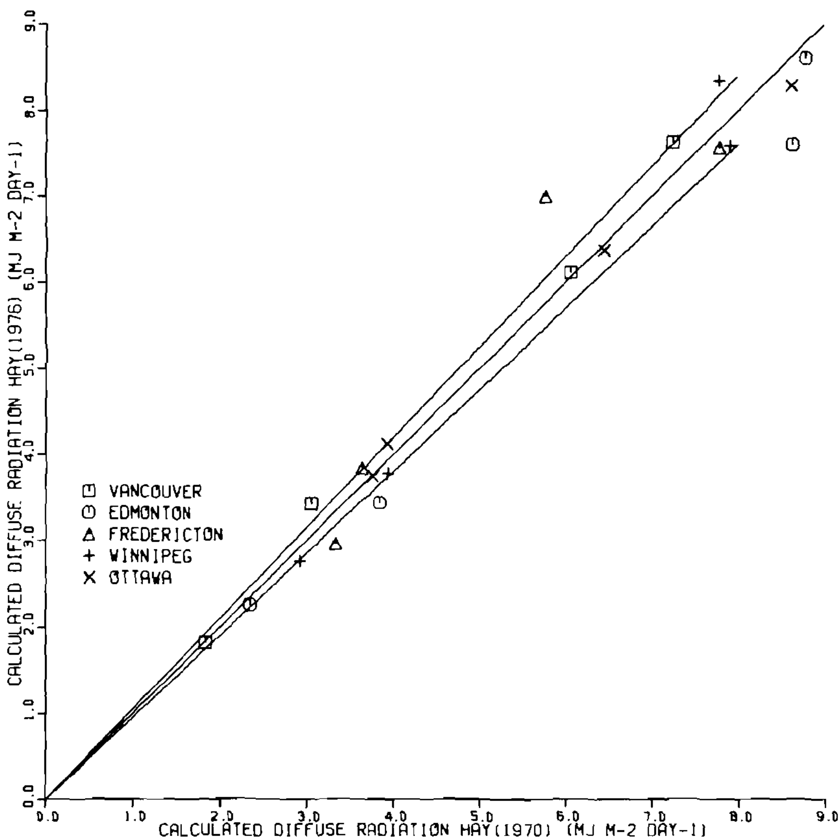

Fig. 5 Comparison of the diffuse short-wave radiation calculated according to Hay (1970) and using the relationship derived in the present study.

of the relationship which allows for multiple reflection, despite the possible inappropriateness of the cloud data.

Hay (1970) has presented maps of the monthly mean total and direct short-wave radiation for Canada from which the relevant data can be obtained for selected locations in order to further test the relationship. The radiation maps are based on calculated rather than observed data but may be considered a totally independent data set with which to test the relationship developed in the present study. Only the "regional" albedos are common to the two approaches since the earlier study calculated the radiation fluxes by the application of appropriate absorption and scattering coefficients to the extraterrestrial radiation.

Fig. 5 presents the results of a comparison of the two independent methods for five locations across southern Canada. The majority of the differences between the two methods are within the indicated limit of 5 per cent, an appropriate accuracy according to Latimer (1972). Thus the widespread regional applicability of the revised relationship is proven.

5 Conclusions

Much of the regional and temporal disparities in the Liu and Jordan type relationship can be attributed to the influence of multiple reflection. With this process taken into account the variability in the relationship is substantially reduced. Its effectiveness in estimating diffuse radiation was evaluated using two independent data sets, with one demonstrating the general regional applicability of the model. The use of constant values for cloud base albedo and the clear sky back-scatterance means that the only additional data requirements are cloud cover and an estimate of "regional" albedo. Given these values, the relationship presented here provides a more general method for calculating the diffuse short-wave radiation from the total short-wave radiation.

Acknowledgments

This study was supported in part by the National Research Council and the Atmospheric Environment Service.

References

ATMOSPHERIC ENVIRONMENT SERVICE. *Monthly radiation summary*. Ottawa: Information Canada.

ATMOSPHERIC ENVIRONMENT SERVICE. 1968. *Climate normals*. Vol. **5** Sunshine, Cloud, Pressure and Thunderstorms. Toronto, 24 pp.

CATCHPOLE, A.J.W. and D.W. MOODIE. 1971. Multiple reflection in Arctic regions. *Weather* **26**: 157–63.

DAVIES, J.A.; W. SCHERTZER; and M. NUNEZ. 1975. Estimating global solar radiation. *Boundary-Layer Meteor*. **9**: 33–52.

DUFFIE, J.A. and W.A. BECKMAN. 1974. *Solar energy thermal processes*. New York: Wiley, 386 pp.

HAY, J.E. 1970. Aspects of the heat and moisture balance of Canada. Ph.D. thesis, University of London, 322 pp.

HUNN, B.D.; G. WILLICUTT; and T. MCSWEENEY. 1975. Simulation and cost optimization of solar heating of buildings in adverse solar regions. Submitted to *Solar Energy*.

KONDRATYEV, K. YA. 1969. *Radiation in the atmosphere*. New York: Academic, 912 pp.

LATIMER, J.R. 1972. *Radiation measurement*. Technical Manual Series No. 2, International Field Year Great Lakes. Ottawa: Information Canada, 53 pp.

LIU, B.Y.H. and R.C. JORDAN. 1960. The interrelationship and characteristic distribution of direct, diffuse and total solar radiation. *Solar Energy* **4**: 1–19.

LÖF, G. and R.A. TYBOUT. 1973. Cost of house heating with solar energy. *Solar Energy* **14**: 253–78.

LONDON, J. 1957. *A study of the atmospheric heat balance*. Report No. AF 19 (122)–165, Dept. of Meteorology and Oceanography. N.Y.: New York University, 75 pp.

MÖLLER, F. 1965. On the backscattering of global radiation by the sky. *Tellus* **17**: 350–5.

RUTH, D.W. and R.E. CHANT. 1976. The relationship of diffuse to total radiation in Canada. *Solar Energy* **18**: 153–4.

SADLER, G.W. 1975. Direct and diffuse insolation using approximation methods applied to horizontal surface insolation. *Solar Energy* **17**: 39–46.

SAWCHUCK, A.M. 1974. The climatology of multiply reflected radiation at Toronto, Canada. M.A. thesis, University of Manitoba, 127 pp.

Seasonal Variability of Rainfall Extremes

Trevor Dickinson
School of Engineering, University of Guelph, Guelph, Ontario

[Manuscript received 7 July 1976; in revised form 1 November 1976]

ABSTRACT

Monthly rainfall extremes have been analyzed for three stations in Southern Ontario. The double exponential probability distribution was fitted to the extreme values for each month considered, each duration selected, and sets of annual extremes. A station-year approach yielded monthly and annual extreme value distributions for the lumped region of Southern Ontario. The analysis has revealed a pronounced seasonal pattern in the rainfall extremes – the amount of rain expected with a selected probability of occurrence during the summer being considerably greater than the rainfall that might be expected to be exceeded at the same probability level during the spring or fall. The extent of the seasonal variability was found also to vary with duration. The implications of the variability are seen to be significant for the estimation of the magnitude and frequency of floods.

1 Introduction

Data regarding extreme rainfalls are often very useful for hydrologists and water resources engineers. Rainfall magnitude and frequency information is used extensively for the prediction of design floods and the probability of occurrence of such flows.

Historically, flood prediction approaches have equated flood frequency to that of the associated rainfall event (Chow, 1962; Spencer and Dickinson, 1970). Researchers have demonstrated that, at least in rural areas, these approaches prove to be problematic as there is virtually no correlation between rainfall and runoff frequencies for selected events (Hiemstra and Reich, 1967; Matheson, 1975). In fact, as the manner in which the watershed system operates upon rainfall input varies dramatically from season to season, relationships between rainfall and runoff frequencies must be dependent upon seasonal variables.

Therefore, to identify aspects of rainfall input relevant to watershed response, it is important to consider the seasonal variability of extreme rainfall characteristics. A method of approaching this task is presented below with reference to data for Southern Ontario.

2 Monthly rainfall extremes

Monthly rainfall extremes of 5-, 10-, 15-, 30-, 60-, 120-, 360-, 720-, and 1440-min durations have been analyzed for three stations in Southern Ontario. The

TABLE 1. Correlation coefficients for Gumbel extremal distributions fitted to monthly and annual rainfall extremes in Southern Ontario

Duration: minutes	Time Interval Apr	May	Jun	Jul	Aug	Sep	Oct	Nov	Year
10	0.975	0.946	0.976	0.990	0.960	0.951	0.977	0.980	0.977
30	0.983	0.949	0.978	0.983	0.952	0.921	0.970	0.984	0.968
60	0.986	0.948	0.966	0.992	0.965	0.912	0.958	0.970	0.978
360	0.978	0.969	0.966	0.973	0.983	0.963	0.960	0.979	0.977
720	9.978	0.978	0.962	0.982	0.988	0.972	0.969	0.980	0.986
1440	0.975	0.987	0.955	0.986	0.979	0.970	9.965	0.982	0.984

monthly extremal information has been available for the months of April through November for London, St Thomas, and Toronto for periods of 35, 50, and 35 years respectively. Data for the winter months of December through March were not analyzed as most precipitation during this season is in the form of snow. Extreme rainfalls in these months are rare and are generally small in comparison to amounts occurring during the rest of the year.

The Gumbel (double exponential) distribution was fitted to the extreme values for each month considered and each duration selected. The sets of annual extremes for the durations at each station were also fitted with the same form of distribution. Fitting was achieved in all cases by the method of moments, and the goodness of fit was examined with regard to both correlation coefficients and control curves. The average correlation coefficients shown in Table 1 reveal that the Gumbel distribution represents yearly and monthly rainfall extremes equally well.

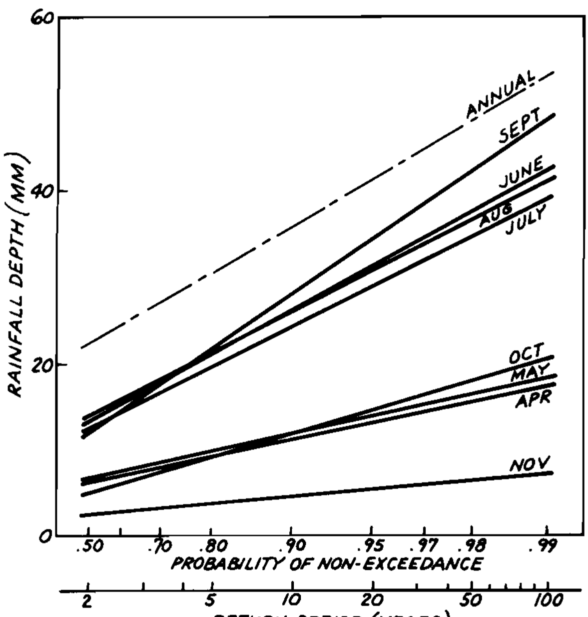

Fig. 1 Monthly and annual extreme value distributions for 30-min storm rainfall at London, Ontario.

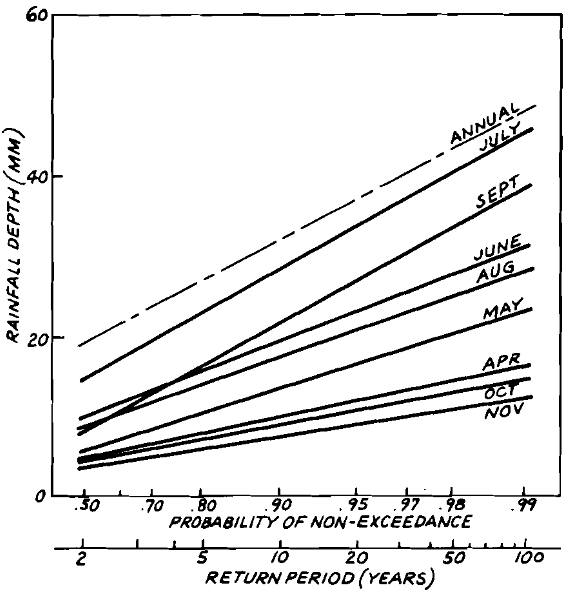

Fig. 2 Monthly and annual extreme value distributions for 30-min storm rainfall at Toronto, Ontario.

Although there has been no attempt in the study to fit other distributions to the rainfall extremes, consideration was given to the σ_1/σ_2 ratio referred to by Jenkinson (1955) and Krishnan and Kushwaha (1975), where σ_1 is the standard deviation of the set of extreme values and σ_2 is the standard deviation of the greater members in pairs of extremes. The Gumbel distribution is most applicable when $\sigma_1 = \sigma_2$, tending to yield overestimates when $\sigma_1 > \sigma_2$ and underestimates when $\sigma_1 < \sigma_2$. Determinations of the ratio for data sets for all months and the range of durations revealed an average ratio of 1.00 and no apparent trends with either season or duration. Sampling errors and the presence of outlier points in the data appeared to be the causes of variations in the ratio. From these results, it follows that the Gumbel distribution should represent the data well.

Examples of the fitted monthly and annual extreme value distributions are presented in Figs 1 and 2. Although the periods of record considered were 35 to 50 years in length, the results revealed considerable scatter attributable to sampling error. In order to reduce such effects, the data for the three locations were combined by means of a station-year approach to yield monthly and annual extreme value distributions for the lumped region of Southern Ontario. An example of these results is presented in Fig. 3.

3 Seasonal variability of parameters

Figs 1, 2, and 3 reveal that for the climatic region studied there is a pronounced seasonal pattern of rain extremes. The return period associated with selected rainfall amounts occurring during the summer months is considerably smaller than that associated with the same amounts occurring during the spring or fall. For example, the return period for a 20 mm rainfall occurring in 30

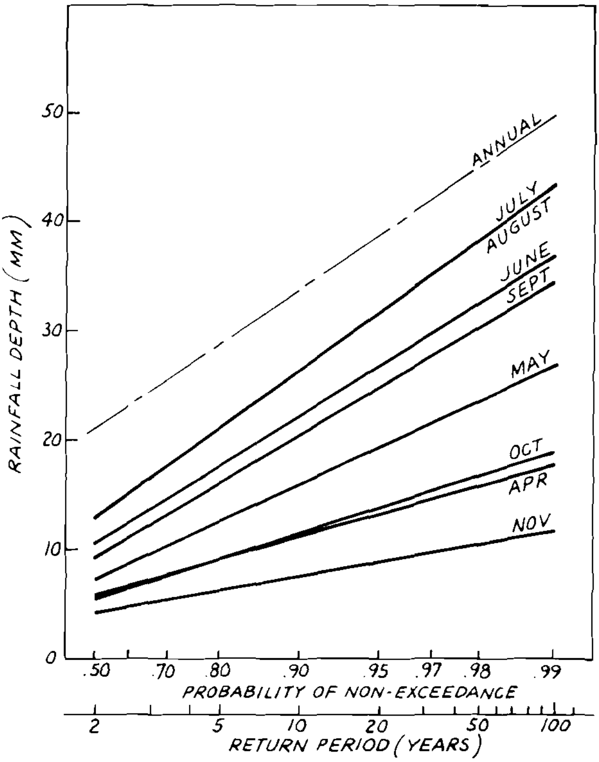

Fig. 3 Monthly and annual extreme value distributions for 30-min storm rainfall in Southern Ontario.

minutes at a point in Toronto during a particular summer month is approximately 10 years; for the same event occurring in a spring or fall month, the return period is >100 years. The amount of rain expected with a selected probability of occurrence during the summer is about double the rainfall that might be expected to be exceeded at the same probability level during the spring and fall.

The seasonal pattern was found to be the same for all durations, with the extent of variability a function of duration. The effect of duration is revealed in the variability of the means and standard deviations of the monthly extremal data, presented in Figs 4 and 5 respectively. The extremal distribution for any selected month and duration may be determined from the relationship,

$$P[X \leqslant x] = e^{-e^{-(a+x)/c}}$$

where $P[X \leqslant x]$ = the probability of the variate X being equal to or smaller than the value x,

$a = 0.450\sigma_x - \mu$,

$c = 0.780\sigma_x$,

μ = the mean of the monthly extreme rainfall, and

σ_x = the standard deviation of the monthly extreme rainfall.

Although the range of seasonal variability among the means appears most peaked for the middle durations in Fig. 4, the ratios of the means in relation to

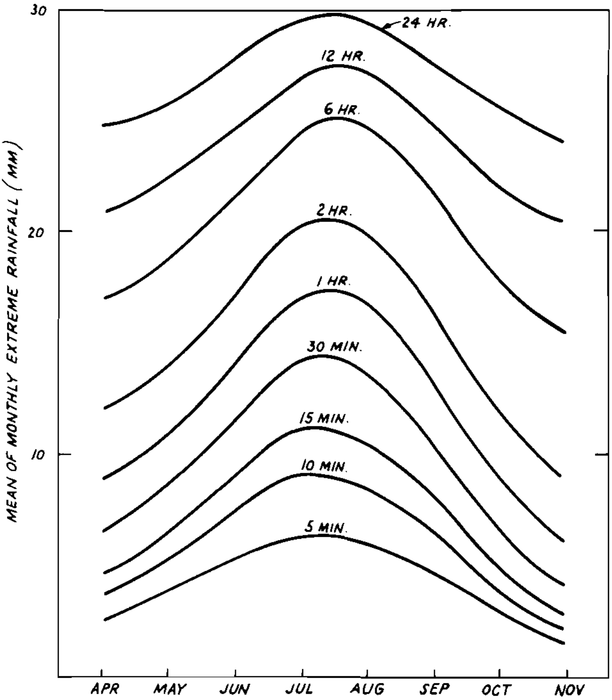

Fig. 4 Means of monthly extreme rainfall distributions for selected storm durations in Southern Ontario.

the April means reveals in Fig. 6 that the range decreases continuously as duration increases. The mean summer extreme rainfall of short duration is more than twice the April mean extreme, while the summer 24 hourly mean extreme is very similar to the April mean.

Fig. 7 reveals that the range in standard deviations of monthly extreme rainfalls is greatest for the 30-, 60-, and 120-min durations. Although the slope of the monthly extremal distributions increases continuously with duration, the range of slopes decreases as duration grows shorter and longer than one hour.

The seasonal pattern in rainfall extremes is attributable to an increase in short-duration convective storm activity during the months of June through September. The pattern in Fig. 7 would also suggest that the storm durations for which this activity is most pronounced is between 30 min and 2 hours. There is also evidence that, for rainfalls occurring in durations of less than 6 hours and during the months of April through November, rainfall extremes are least in November.

The seasonal variability of extremes in conjunction with storm duration can be summarized in the form of monthly depth vs duration curves for selected return periods. An example of this format is shown in Fig. 8.

4 Annual extremes from monthly data

If a year is considered to be composed of monthly intervals, and if for each interval there exists an independent extremal probability distribution for rain-

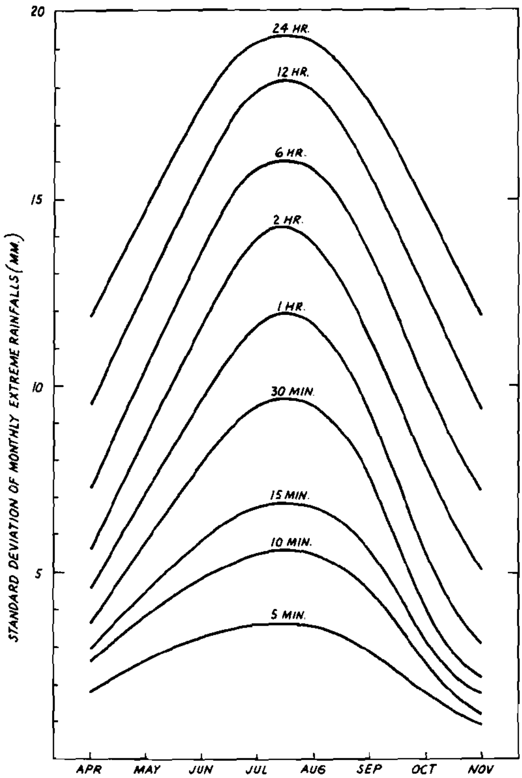

Fig. 5 Standard deviations of monthly extreme rainfall distributions for selected storm durations in Southern Ontario.

fall amounts occurring in specific durations, the probability of a selected rainfall event not being exceeded in a year may be expressed as the product of the monthly non-exceedance probabilities. That is,

$$P_y[X < x] = P_1[X < x] \times P_2[X < x] \times \ldots \times P_n[X < x]$$
$$= \prod_{i=1}^{n} P_i[X < x] \tag{1}$$

where $P_y[X < x]$ = the probability of x not being exceeded in a year, i.e. n time intervals, and

$P_i[X < x]$ = the probability of x not being exceeded in the ith time interval.

Then the probability of x being equalled or exceeded in a year may be expressed,

$$P_y[X \geqslant x] = 1 - \prod_{i=1}^{n} P_i[X < x]\,. \tag{2}$$

When monthly rainfall extremes are represented with the Gumbel distribution, the probability of a selected rainfall event being equalled or exceeded in a year may then be expressed,

$$P_y[X \geqslant x] = 1 - \prod_{i=1}^{n} e^{-e^{-(x+a_i)/c_i}} \tag{3}$$

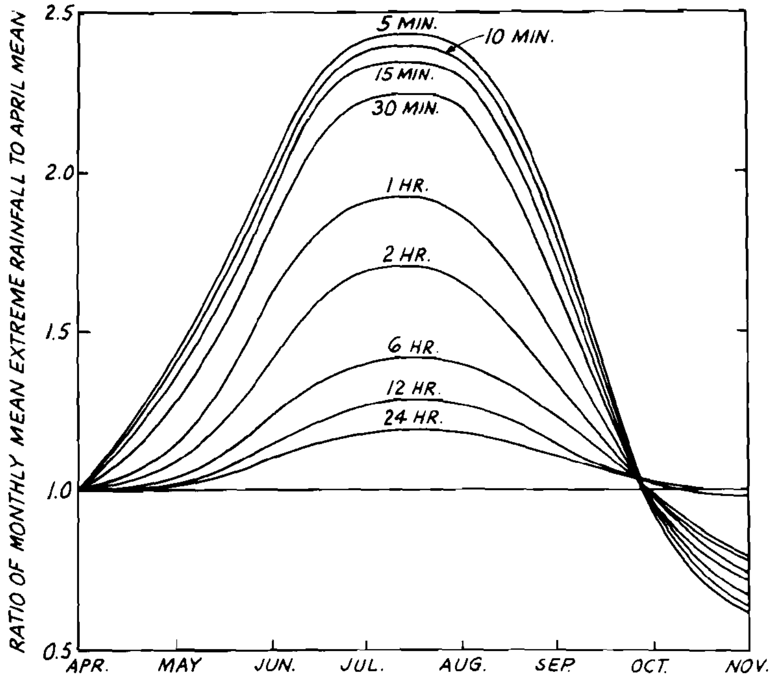

Fig. 6 Ratios of monthly mean extremes for selected storm durations in Southern Ontario.

where a_i, c_i = the parameters of the Gumbel double exponential distribution representing the extremes in the ith time interval.

This approach was employed to estimate the distribution of annual rainfall extremes for each duration considered at the Southern Ontario stations. Examples of the results are shown in Figs 1, 2, 3, and 8.

The annual extremal distributions developed with expression (3) are not of double exponential form. However, except for data sets in which serious outliers exist, these distributions closely approximate double exponential distributions fitted to annual extremes. Where outliers do exist, the approach involving expression (3) greatly reduces the effect of outliers on the estimated annual distribution.

5 Summary comments

Short-duration convective storm activity during the summer months causes a pronounced seasonal pattern in extreme rainfall amounts in Southern Ontario. The amount of rain expected with a selected probability of occurrence during the summer is considerably greater than the rainfall that might be expected to be exceeded at the same probability level during the spring or fall. Although the pattern is similar for all storm durations from 5 minutes to 24 hours, the extent of the seasonal variability varies with duration. Variations in slope of the monthly extreme rainfall relationships are greatest for a storm duration of one hour.

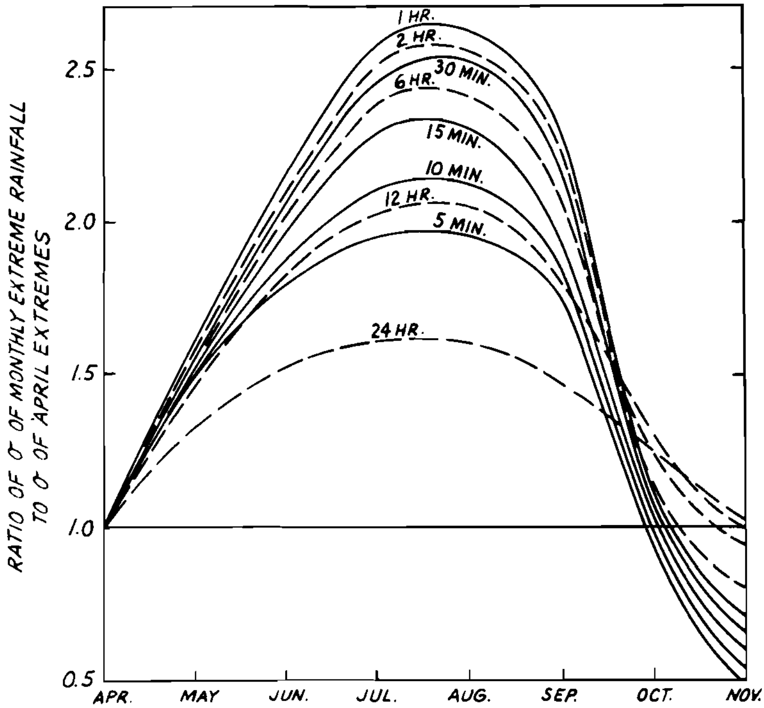

Fig. 7 Ratios of monthly standard deviations of extremes for selected storm duration in Southern Ontario.

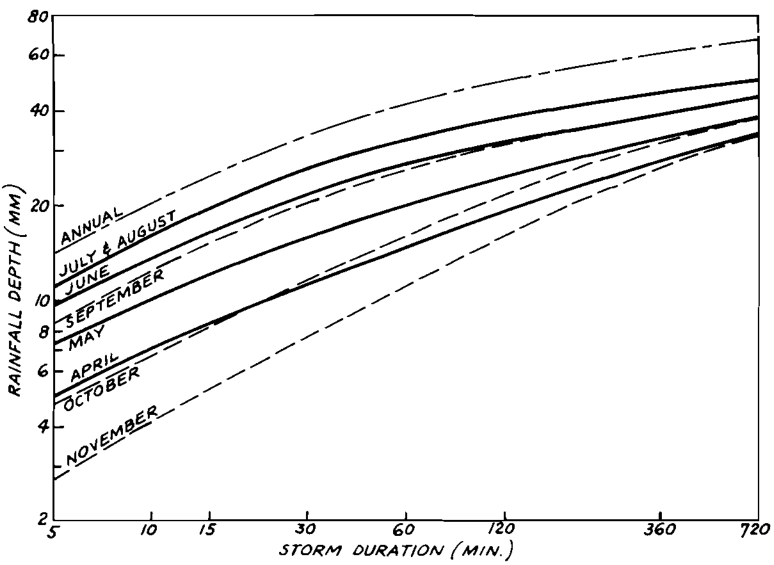

Fig. 8 Monthly depth vs duration curves for storms of 10-year return period in Southern Ontario.

The implications of this seasonal variability are significant for the estimation of flood peaks and their frequency of occurrence. Although rainfall extremes are most likely to occur during the summer months, peak streamflow in Southern Ontario occurs most frequently during the winter and spring period. Therefore, watershed moisture and cover conditions significantly moderate summer rainfalls but exert a much smaller effect on spring storms. Information regarding the nature of rainfall extremes in the spring months may lead to improved understanding and prediction of the runoff vs rainfall relationships not only during that period but also throughout the year.

Acknowledgments

The author wishes to acknowledge the analytical assistance and useful suggestions of Mr Alex Matheson and Prof. Hugh Whiteley. The National Research Council of Canada has supported the research activity through a Grant-in-Aid-of-Research, and the Ontario Ministry of Agriculture and Food has provided financial assistance under Research Program 33 — Resources Inventory, Planning, and Development.

References

CHOW, V.T. 1962. *Hydrologic determination of waterway areas for the design of drainage structures in small drainage basins.* Univ. of Illinois Eng. Expt. Sta. Bull. No. 462.

HIEMSTRA, L.A.V. and B.M. REICH. 1967. *Engineering judgement and small area flood peaks.* C.S.U. Hydrology Paper 19, Fort Collins.

JENKINSON, A.F. 1955. The frequency distribution of the annual maxima values of meteorological elements. *Quart. J. Roy. Meteor. Soc.* **81**: 158–71.

KRISHNAN, A. and R.S. KUSHWAHA. 1975. Comparison of Gumbel and Jenkinson's methods of estimating probable maximum rainfall intensities over India for different return periods. *Cent. Brd Irrig. and Power J.*: 223–35.

MATHESON, A.D. 1975. Estimation of runoff probabilities. University of Guelph M.Sc. thesis.

SPENCER, V.I.D. and W.T. DICKINSON. 1970. *Farm pond design in Ontario.* Toronto: Ontario Dept of Agriculture and Food.

CALL FOR PAPERS – ELEVENTH ANNUAL CONGRESS

The Eleventh Annual Congress and Annual General Meeting of the Canadian Meteorological Society will be held at the Winnipeg Convention Centre, Winnipeg, Manitoba on 1–2–3 June 1977. The weather and climate of the plains areas of Canada and the United States will be explored in the congress theme, "The Meteorology of the Great Plains." Sessions are also planned on physical meteorology, weather forecasting, micrometeorology, hydrometeorology, agricultural and forest meteorology, air pollution, and other topics according to the papers submitted.

The Oceanography Division of the Society will be featuring the Canadian Arctic, with additional sessions on limnology, estuaries and coastal processes, and offshore oceanography. Contributions related to these areas are invited from all branches of oceanography and limnology. Contributions from biological, chemical and geological oceanographers, and limnologists are particularly encouraged. Invited speakers will present overview papers at the start of each session.

Titles and definitive abstracts of up to 300 words should reach the Program Committee no later than 15 February 1977. Meteorological papers should be sent to Mr Hugh M. Fraser, Atmospheric Environment Service, 600 – 185 Carlton Street, Winnipeg, Manitoba R3C 3J1. Oceanographic contributions should be addressed to Dr Noel Boston, Beak Consultants, Ste 602 – 1550 Alberni Street, Vancouver, B.C. V6G 1A5.

The congress will use the modern facilities of the Winnipeg Convention Centre with accommodation in convenient hotels. Further information will appear in the Society's journal *Atmosphere* or may be obtained from the Congress Coordinator, Mr A.H. Lamont, Atmospheric Environment Service, 600 – 185 Carlton Street, Winnipeg, Manitoba R3C 3J1.

SOLLICITATION DE PAPIERS – ONZIÈME CONGRÈS

Le onzième congrès annuel et l'assemblée générale annuelle de la Société météorologique du Canada se tiendra au Centre des conventions à Winnipeg au Manitoba, les 1–2–3 juin 1977. Le temps et le climat des plaines du Canada et des Etats Unis seront étudiés dans le cadre du thème "La Météorologie des Grandes Plaines." Des séances sur la météorologie physique, la prévision du temps, la micrométéorologie, l'hydrométéorologie, la météorologie forestière et agricole, la pollution de l'air sont également prévues. D'autres sujets seront inclus suivant les papiers soumis.

La Division océanographique de la Société aura comme sujet principal l'arctique canadien. Des séances supplémentaires porteront sur la limnologie, sur les processus relatifs aux estuaires et aux littoraux et également sur l'océanographie au large des côtes. Nous invitons toutes les composantes de l'océanographie et de la limnologie à participer par des contributions dans les domaines précités. On encourage plus particulièrement les océanographes spécialistes en biologie, en chimie et en géologie ainsi que les limnologistes à participer. Les conférenciers invités présenteront des synthèses de leurs domaines d'activité au début de chaque séance.

Les titres et les résumés définitifs contenant jusqu'à 300 mots devront parvenir au Comité du programme avant le 15 février 1977. La documentation météorologique devra être envoyée à M. Hugh M. Fraser, Service de l'environnement atmosphérique, 600–185 rue Carlton, Winnipeg, Manitoba R3C 3J1. Les papiers sur l'océanographie devront être adressés au Dr Noel Boston, Beak Consultants, Ste 602–1550 rue Alberni, Vancouver, British Columbia V6G 1A5.

Le congrès utilisera les installations modernes du Centre des conventions de Winnipeg et les invités seront hébergés dans des hotels avoisinants. De plus amples renseignements seront donnés dans le périodique de la Société, *Atmosphère*. On peut également s'informer auprès du Coordonnateur, M. A.H. Lamont, Service de l'environnement atmosphérique, 600–185 rue Carlton, Winnipeg, Manitoba R3C 3J1.

Modelling Direct, Diffuse, and Total Solar Radiation for Cloudless Days

P.W. Suckling
and
J.E. Hay
Department of Geography, University of British Columbia, Vancouver

[Manuscript received 14 June 1976; in revised form 1 October 1976]

ABSTRACT

A simple form of solar radiation model was analysed for cloudless days for Goose, Nfld., Port Hardy, B.C., and Edmonton, Alta. Performance for daily values of total solar radiation was satisfactory; however, data for Goose indicated that the model over- and under-estimated the direct and diffuse components of solar radiation, respectively. Modifications, including solving for an aerosol parameter k and substituting 0.6 forward scattering instead of the more commonly used 0.5, improved model performance for direct and diffuse radiation.

1 Introduction

Recently, interest in the spatial distribution of solar radiation has increased especially with respect to the potential utilization of solar energy (Chant and Ruth, 1975; Hay, 1975). It has been shown that interpolation of solar radiation values from existing measuring stations can result in significant errors (Wilson and Petzold, 1972; Suckling and Hay, 1976). An alternative is the numerical model utilizing standard synoptic weather data available for numerous locations and this approach must be implemented in order to supplement the available solar radiation data.

Based on the original work of Houghton (1954), several researchers have developed and utilized a simple model for the estimation of solar radiation incident on a horizontal surface under cloudless skies (Monteith, 1962; Idso, 1969, 1970; Hay, 1970a; Davies et al., 1975). The model was shown to perform well in these studies. However, some applications in the fields of solar energy and air pollution studies among others require the knowledge of the direct and diffuse components of the total solar radiation separately. It is the purpose of this paper to report on the performance of the Houghton model in this regard and on the modifications required to obtain reasonable estimates of the direct and diffuse components.

2 Solar radiation model

On cloudless days, solar radiation received at the surface ($K\downarrow$) is the residual of the extraterrestrial radiation at the top of the atmosphere, depleted by atmospheric absorption and scattering. As shown in previous studies (Idso, 1969; Hay, 1970a; Davies et al., 1975) the direct beam radiation, S, at the surface can be expressed as:

$$S = I_0 \cos Z\, \psi_{wa}\psi_{da}\psi_{ws}\psi_{rs}\psi_{ds}\,, \tag{1}$$

where I_0 is the solar constant (1353 W m^{-2}, Thekaekara and Drummond, 1971), Z is the solar zenith angle and the ψ terms are transmission functions after water vapour absorption, aerosol or dust absorption, water vapour scattering, Rayleigh scattering, and aerosol or dust scattering respectively. Following Houghton (1954), absorption of the solar beam was assumed to occur before scattering and half of the aerosol or dust depletion was assumed to be due to absorption.

The scattered portion of the direct beam reaching the ground, D_s, can be expressed as follows, assuming half of the scattered radiation reaches the surface:

$$D_s = 0.5\, I_0 \cos Z\, \psi_{wa}\psi_{da}(1 - \psi_{ws}\psi_{rs}\psi_{ds}). \tag{2}$$

An additional term representing the first order component of the multiply-reflected radiation, D_b, was added following the work of Hay (1970a):

$$D_b = \alpha(S + D_s)\ (0.5\, \psi_{wab}\psi_{dab}(1 - \psi_{wsb}\psi_{rsb}\psi_{dsb})), \tag{3}$$

where α is the surface reflection coefficient or albedo and the b subscripts in the ψ terms represent the transmissions for diffuse radiation with optical air mass m = 1.66. Albedo was assumed to be 0.2 with no snow cover and 0.8 with snow. Equation (3) represents the first term of a geometric series. Therefore,

$$D_b = (S + D_s)\ \rho/(1 - \rho), \tag{3a}$$

where

$$\rho = 0.5\, \alpha\psi_{wab}\psi_{dab}(1 - \psi_{wsb}\psi_{rsb}\psi_{dsb}). \tag{3b}$$

For computation, the first order term given by equation (3) was used. The incoming diffuse radiation ($D{\downarrow}$) is the sum

$$D{\downarrow} = D_s + D_b, \tag{4}$$

and global radiation is the sum of the direct and diffuse components:

$$K{\downarrow} = S + D{\downarrow}. \tag{5}$$

The transmission functions used are those expressed by Davies et al. (1975) as follows:

$$\psi_{rs} = 0.972 - 0.08262m + 0.00933m^2 - 0.00095m^3 + 0.0000437m^4, \tag{6}$$

$$\psi_{ws} = 1 - 0.0225mu, \tag{7}$$

$$\psi_{wa} = 1 - 0.077(mu)^{0.3}, \tag{8}$$

and

$$\psi_D = \psi_{da}\psi_{ds} = \kappa^m, \tag{9}$$

where m is the optical air mass, u is precipitable water in centimetres and κ is an aerosol or dust parameter. The formulations for ψ_{rs} and ψ_{ws} are from Houghton's original curves. The optical air mass was calculated for hourly periods using the formulation of Kasten (1966) for relative optical air mass, m_r:

$$m_r(Z) = 1/[\cos Z + 0.15(93.885 - Z)^{-1.253}], \tag{10}$$

and then corrected for pressure, p (in mb), as:

$$m(Z) = \frac{m_r(Z)p}{1013.25}. \tag{11}$$

Precipitable water u was calculated using 0000 and 1200 h GMT radiosonde observations by the method of Hay (1970b). The formulation for ψ_{wa} is that proposed by McDonald (1960). For the aerosol or dust term, Houghton (1954) assumed equality between ψ_{da} and ψ_{ds},

$$\psi_{da} = \psi_{ds} = k^m, \tag{12}$$

where k was given the value 0.975. This corresponds to $\kappa = 0.95$ in (9).

3 Performance of the unmodified solar radiation model

Hourly meteorological data from the Atmospheric Environment Service of Canada were analysed for each of the following locations: Goose, Nfld., Port Hardy, B.C., and Edmonton, Alta. The available period of record is indicated in Table 1. These stations were chosen as a consequence of the availability of surface hourly, upper air, and radiation data and because of a desire for locations representative of contrasting atmospheric environments. Days with cloudless skies during the daylight periods were identified with allowance for up to four hourly observations of one-tenth cloud cover being accepted as "cloudless." Table 2 lists the days utilized both for model development and subsequent independent testing.

TABLE 1. Locations and periods of available data record used in this study

	Goose	Port Hardy	Edmonton
Latitude	53°19′N	50°41′N	53°34′N
Longitude	60°25′W	127°22′W	113°31′W
Period of available data record	1964–1975	1968–1972	1960–1971

Modelled values of solar radiation were calculated for hourly periods and summed to obtain daily totals for the first group of days for each location. These hourly and daily totals were compared to measured values as reported in the *Monthly Radiation Summary* (Atmospheric Environment Service, Toronto, Canada). Model performance is summarized in Table 3 using both

TABLE 2. "Cloudless" days utilized in this study

(a) Model Development:

Goose	Port Hardy	Edmonton
Jan. 8 1964	Jan. 26 1968	Aug. 9 1960
Jan. 19 1964	Feb. 9 1968	Nov. 27 1960
Mar. 11 1964	Feb. 12 1968	Mar. 18 1961
Mar. 14 1964	Feb. 15 1968	Sept. 13 1961
Apr. 20 1964	Feb. 27 1968	Sept. 14 1961
Jan. 24 1965	Mar. 6 1969	May 21 1963
Jan. 6 1966	Mar. 10 1969	May 22 1963
Mar. 18 1966	Mar. 11 1969	Sept. 28 1963
May 17 1966	Oct. 13 1969	Oct. 7 1964
Jan. 24 1967	Jan. 16 1970	Oct. 8 1964
Feb. 3 1967	Mar. 1 1970	Feb. 2 1965
Apr. 7 1967	Mar. 9 1970	Mar. 19 1965
Dec. 11 1967	July 27 1971	Dec. 13 1965
Jan. 31 1968	July 29 1971	Jan. 19 1966
Mar. 21 1968	Oct. 27 1971	May 6 1966
		May 8 1966
		Aug. 22 1966
		Sept. 17 1967
Total # days: 15	15	18

(b) Independent testing:

Goose	Port Hardy	Edmonton
Jan. 6 1969	May 6 1972	Feb. 10 1968
Feb. 24 1969	Oct. 12 1972	May 19 1968
Feb. 26 1969	Oct. 16 1972	Nov. 7 1968
Feb. 27 1969	Nov. 15 1972	June 8 1969
Feb. 17 1971	Dec. 3 1972	Oct. 17 1969
Feb. 23 1971		Oct. 30 1970
Feb. 20 1973		Nov. 4 1970
Mar. 2 1973		Nov. 22 1970
Jan. 26 1974		May 12 1971
Mar. 9 1974		July 29 1971
Apr. 28 1974		
Feb. 22 1975		
Total # days: 12	5	10

relative and absolute values of the root mean square error and the average bias error. The latter is included in the RMS errors. Daily performance is shown in Fig. 1. Considering that measurement errors for solar radiation are commonly 5 per cent of the measured flux (Latimer, 1972), Table 3 indicates that the accuracy of this model for daily totals of $K\downarrow$ is acceptable. The root mean square error values of less than 1.5 MJ m^{-2} day^{-1} are considerably less than the average expected differece of at least ± 3.5 MJ m^{-2} day^{-1} found by Suckling and Hay (1976) for extrapolations of measured solar radiation over distances of greater than 250 km. This latter study involved days with all sky conditions whereas the present study is for cloudless days only. Although greater relative errors are expected when considering all conditions, cloudless days tend to have high incident radiation and hence small relative errors might

TABLE 3. Performance of unmodified Houghton model for model development days

(a) Daily Totals:

Location	Radiation Component	Root Mean Square Error ($MJm^{-2} day^{-1}$)	Root Mean Square Error (Percentage)	Average Per cent Deviation From Measured
Goose	$K\downarrow$	0.56	4.3	0.0
Goose	S	0.76	7.5	4.7
Goose	$D\downarrow$	0.72	23.6	−13.3
Port Hardy	$K\downarrow$	0.97	7.3	+4.9
Edmonton	$K\downarrow$	1.45	8.2	−0.9

(b) Hourly Values:

Location	Radiation Component	Root Mean Square Error ($KJ\ m^{-2} h^{-1}$)
Goose	$K\downarrow$	75.3
Goose	S	92.9
Goose	$D\downarrow$	73.4
Port Hardy	$K\downarrow$	128.5
Edmonton	$K\downarrow$	134.5

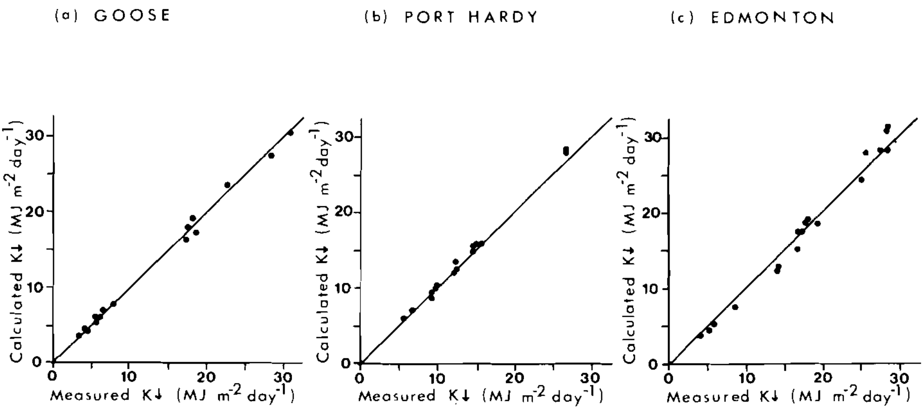

Fig. 1 Daily performance of the unmodified Houghton solar radiation model for model development days.

still create large absolute errors. Despite the above, this study shows that the model yields errors of small absolute magnitude. In relative terms, errors of less than 10% for daily totals of $K\downarrow$ (including the average bias) were found. Further work is to be carried out modelling solar radiation under all sky conditions which will provide a more direct comparison with the extrapolation errors discussed by Suckling and Hay (1976).

Diffuse radiation values were available only for Goose. The direct component is calculated as the difference between $K\downarrow$ and $D\downarrow$. As shown in Table 3, daily totals of S and $D\downarrow$ were over- and under-estimated respectively. In fact,

S was over-estimated for all but two days and $D\downarrow$ under-estimated in all but one case and the root mean square error values were generally larger than those for $K\downarrow$. It can be seen that the deviations between calculated and measured values of S and $D\downarrow$ are large and systematic and therefore modifications are necessary to improve estimates of these components.

4 Modified solar radiation model

The partitioning of solar radiation between its direct and diffuse components can be effected by aerosol or dust scattering and absorption. The value of k in (12) was therefore evaluated for hourly periods for Goose by solving for $\psi_d (= \psi_{da} = \psi_{ds})$ in (1),

$$\psi_d = \left(\frac{S}{I_0 \cos Z \psi_{wa} \psi_{ws} \psi_{rs}} \right)^{1/2}. \tag{13}$$

The hourly values of k were weighted according to the incident S when determining daily mean values. The average of these daily values for the days indicated in Table 2(a) was 0.965 with a range of 0.947 to 0.977. The calculated values of k are thus generally lower than the previously assumed value of 0.975. The use of the new value of k naturally leads to an accurate estimate of S on an average while the diffuse radiation was still under-estimated, but in this case by 12% or with a root mean square error of 0.66 MJ m^{-2} day^{-1}.

The unmodified model assumed that forward- and back-scattering were equal and thus half of the scattered radiation reaches the ground as diffuse radiation. While this is true of molecular scattering, scattering by other aerosol particles is directed preferentially forward (Robinson, 1963). With $k = 0.965$ for Goose,

TABLE 4. Performance of the modified model for model development days

(a) Daily Totals:

Location	Radiation Component	Root Mean Square Error (MJ m^{-2} day^{-1})	Root Mean Square Error (Percentage)	Average Per cent Deviation From Measured
Goose	$K\downarrow$	0.64	4.9	−2.1
Goose	S	0.51	5.1	−2.1
Goose	$D\downarrow$	0.48	15.7	−2.9
Port Hardy	$K\downarrow$	0.57	4.3	−1.1
Edmonton	$K\downarrow$	1.36	7.7	−3.4

(b) Hourly Values:

Location	Radiation Component	Root Mean Square Error (KJ m^{-2} h^{-1})
Goose	$K\downarrow$	78.2
Goose	S	68.7
Goose	$D\downarrow$	49.4
Port Hardy	$K\downarrow$	97.7
Edmonton	$K\downarrow$	130.6

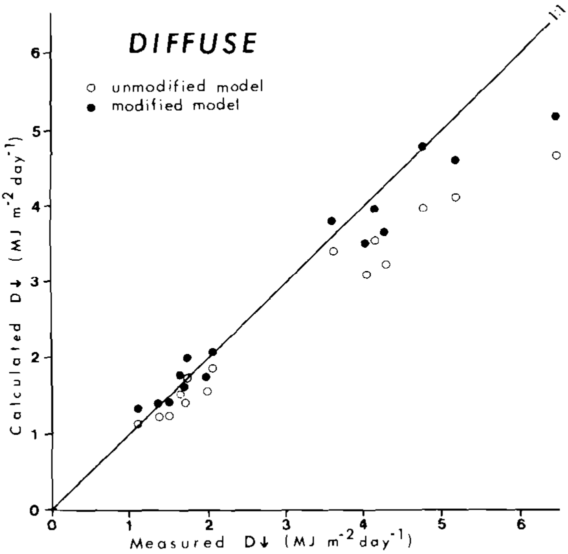

Fig. 2 Measured and calculated values of diffuse solar radiation from the unmodified and modified models for Goose for model development days.

the ratio of forward- to back-scattering was varied in order to determine the value which minimized the error in the estimate of the diffuse radiation. Values of 0.6 forward- and 0.4 back-scattering in place of 0.5 in (2) and (3), respectively, tended to improve model accuracy. Lettau and Lettau (1969) have used values of forward- and back-scattering of ⅔ and ⅓, which are not dissimilar from the revised values considered here.

Table 4 shows the performance of this modified model. For Goose, compared with the unmodified model (Table 3), the revised model shows a small deterioration in $K\downarrow$ estimation. However, substantial improvement is seen for both S and $D\downarrow$. Fig. 2 indicates the improved performance of the modified model in estimating daily values of cloudless sky diffuse solar radiation at Goose.

In order to apply the modified model to stations without diffuse radiation data, a method for determining the aerosol parameter k in equation (12) from $K\downarrow$, rather than S must be developed. For a dust-free atmosphere (indicated by a prime in the following equations),

$$S' = I_0 \cos Z\, \psi_{wa}\psi_{ws}\psi_{rs}, \tag{14}$$

$$D'_s = 0.6\, I_0 \cos Z\, \psi_{wa}(1 - \psi_{ws}\psi_{rs}), \tag{15}$$

$$D'_b = \alpha(S' + D'_s)\ (0.4\, \psi_{wab}(1 - \psi_{wsb}\psi_{rsb})). \tag{16}$$

Therefore, the value of the dust-free cloudless sky global radiation is

$$K\downarrow' = S' + D'_s + D'_b. \tag{17}$$

A combination of (4), (5), and (17) can be used to derive a ratio X as

$$X = \frac{K\downarrow}{K\downarrow'} = \frac{S + D_s + D_b}{S' + D'_s + D'_b}. \tag{18}$$

To facilitate computations, the first order component of the multiply-reflected radiation was omitted. Therefore,

$$X \doteq \frac{S + D_s}{S' + D'_s}. \tag{19}$$

Substituting from equations (1), (2), (14), and (15) into equation (19),

$$\begin{aligned} X = (&I_0 \cos Z\, \psi_{wa}\psi_{ws}\psi_{rs}\psi_d^2 + 0.6\, I_0 \cos Z\, \psi_{wa}\psi_d \\ &-0.6\, I_0 \cos Z\, \psi_{wa}\psi_{ws}\psi_{rs}\psi_d^2) \,/\, (I_0 \cos Z\, \psi_{wa}\psi_{ws}\psi_{rs} \\ &+ 0.6\, I_0 \cos Z\, \psi_{wa} - 0.6\, I_0 \cos Z\, \psi_{wa}\psi_{ws}\psi_{rs}). \end{aligned} \tag{20}$$

If Y represents the denominator of equation (20),

$$X = \left(\frac{I_0 \cos Z\psi_{wa}\psi_{ws}\psi_{rs} - 0.6 I_0 \cos Z\psi_{wa}\psi_{ws}\psi_{rs}}{Y}\right) \psi_d^2 + \left(\frac{0.6 I_0 \cos Z\psi_{wa}}{Y}\right) \psi_d, \tag{21}$$

which is in the form of a quadratic equation. Solving this, a positive value of ψ_d can be determined and then substituted into (12) to obtain hourly values of the aerosol parameter k. Mean daily values were then calculated weighted according to incident $K\downarrow$. With this method, an average daily value of $k = 0.965$ for the 15 days was again obtained for Goose, indicating that the decision to omit the first order component of the multiply-reflected radiation in the calculation of k does not generally invalidate this approach.

The same method, with the multiple reflection terms omitted, was also used to evaluate average values of k for Port Hardy and Edmonton. Values of 0.95 (with a range in mean daily values of 0.924 to 0.965) and 0.96 (range 0.915 to 0.977) were obtained for these two locations, respectively. Davies et al. (1975) obtained a value of $\kappa = 0.88$ which results in, through (9) and (12), a value for k of 0.94 for the Lake Ontario area. Lower values in their study compared to the stations reported here are consistent with the general higher level of atmospheric pollution associated with the high concentration of industrial activity in the southern Ontario region. With the appropriate mean values of k and a forward scattering factor of 0.6, $K\downarrow$ was calculated for Port Hardy and Edmonton. It is necessary to assume a value for this latter factor in the absence of diffuse radiation data for Port Hardy and Edmonton. Thus, the value of 0.6 used for Goose was assigned. Although absent in the calculation of k, the multiple reflection term is again included in the final

TABLE 5. Performance of the unmodified and modified models on independent data

(a) Daily Totals:

Location	k for modified model	Radiation Component	Root Mean Square Errors unmodified ($MJ\ m^{-2}\ day^{-1}$)	unmodified (%)	modified ($MJ\ m^{-2}\ day^{-1}$)	modified (%)	Average Per cent Deviation from Measured unmodified	modified
Goose	0.965	$K\downarrow$	0.83	7.0	0.63	5.3	+5.5	+3.4
Goose	0.965	S	0.97	10.6	0.59	6.4	+9.5	+2.8
Goose	0.965	D	0.31	11.4	0.37	13.7	−4.6	+7.3
Port Hardy	0.95	$K\downarrow$	0.67	5.3	0.41	3.4	+2.5	−4.2
Edmonton	0.96	$K\downarrow$	2.06	13.4	1.77	11.5	+8.6	+5.8

(b) Hourly Values:

Location	k for modified model	Radiation Component	Root Mean Square Errors ($KJ\ m^{-2}\ h^{-1}$) unmodified	modified
Goose	0.965	$K\downarrow$	99.6	82.4
Goose	0.965	S	117.5	82.5
Goose	0.965	D	41.9	46.6
Port Hardy	0.95	$K\downarrow$	78.3	60.3
Edmonton	0.96	$K\downarrow$	188.7	167.4

calculation of the radiation fluxes and is thus comparable to the calculations for Goose. Performance of this modified model for these stations is also shown in Table 4. Whereas the modified model showed slight deterioration for $K\downarrow$ estimation at Goose, comparison of Tables 4 and 3 indicates slight reductions in the root mean square errors, both in absolute and relative terms, for Edmonton and substantial reductions for Port Hardy.

5 Independent data tests

The cloudless days listed in Table 2(b) were used to test the modified model with independent data from each of the three locations. The values of k found in section 4 were used for the modified model, and for comparison, the unmodified model discussed in section 3 was also used to evaluate solar radiation for these days. The performance of these two models for $K\downarrow$, S, and $D\downarrow$ estimation at Goose and for $K\downarrow$ estimation at both Port Hardy and Edmonton is summarized in Table 5. For both daily totals and hourly values, root mean square errors for the modified model were generally less and in some situations appreciable reductions in error were achieved. This indicates that the above modifications are advantageous. One exception is for diffuse radiation estimation at Goose where a deterioration occurred in the independent testing of the modified model, despite substantial improvement in the initial testing of the same model.

6 Conclusion

A simple form of the solar radiation model for cloudless skies based on the original work of Houghton (1954) performed well for daily totals of solar radiation for Goose, Nfld., Port Hardy, B.C., and Edmonton, Alta. However, values of direct and diffuse radiation were over-estimated and under-estimated respectively for Goose, Nfld. Modifications including solving for the aerosol parameter k and substituting 0.6 forward scattering for the original 0.5 assumption improved model performance considerably for both hourly and daily values of direct and diffuse solar radiation, except as noted in section 5. Slight improvements in total solar radiation estimation were also evident for Port Hardy and Edmonton. Tests on independent data confirmed the usefulness of the previously calculated k values. These modifications may not be warranted when considering total solar radiation only; however, the above results indicate that they are certainly advantageous when the direct and diffuse components are desired.

In order to use this model, a value of k in (12) must first be chosen. Based on this study, a value somewhat lower than Houghton's 0.975 would seem to be appropriate. With knowledge of air mass (from (10) and (11)) and precipitable water, the direct and diffuse components of solar radiation can be found utilizing (1) through (4) and the total solar radiation from (5).

Subsequent work to extend this model will involve the incorporation of days with cloud under a variety of synoptic regimes.

Acknowledgments

Research funds were supplied, in part, by the Atmospheric Environment Service, which also supplied data, and the National Research Council of Canada.

References

CHANT, R.E. and D.W. RUTH. 1975. Solar heating in Canada. In *The potential of solar energy for Canada*, Conference of the Solar Energy Society of Canada Inc., ed. R.K. Swartman. Ottawa, pp. III 1–10.

DAVIES, J.A.; W. SCHERTZER; and M. NUNEZ. 1975. Estimating global solar radiation. *Boundary-Layer Meteor.* **9**: 33–52.

HAY, J.E. 1970a. *Aspects of the heat and moisture balance of Canada.* Ph.D. thesis, University of London, 2 vols., 322 pp.

——— 1970b. Precipitable water over Canada. I Computation. *Atmosphere* **8**: 128–43.

——— 1975. Solar energy utilization in Canada: a climatological perspective. In *The potential of solar energy for Canada*, Conference of the Solar Energy Society of Canada Inc., ed. R.K. Swartman. Ottawa, pp. I 23–40.

HOUGHTON, H.G. 1954. On the annual heat balance of the northern hemisphere. *J. Meteor.* **11**: 1–9.

IDSO, S.B. 1969. Atmospheric attenuation of solar radiation. *J. Atmos. Sci.* **26**: 1088–95.

——— 1970. The transmittance of the atmosphere for solar radiation on individual clear days. *J. Appl. Meteor.* **9**: 239–41.

KASTEN, F. 1966. A new table and approximation formula for the relative optical air mass. *Arch. Meteor. Geophy. Bioklim.* B **14**: 206–23.

LATIMER, J.R. 1972. *Radiation measurement.* Technical Manual Series No. 2, International Field Year Great Lakes. Ottawa, 53 pp.

LETTAU, H. and K. LETTAU. 1969. Short-wave radiation climatonomy. *Tellus* **21**: 208–22.

MCDONALD, J.E. 1960. Direct absorption of solar radiation by atmospheric water vapour. *J. Meteor.* **17**: 319–28.

MONTEITH, J.L. 1962. Attenuation of solar radiation: a climatological study. *Quart. J. Roy. Meteor. Soc.* **88**: 508–21.

ROBINSON, G.D. 1963. Absorption of solar radiation by atmospheric aerosol, as revealed by measurements at the ground. *Arch. Meteor. Geophy. Bioklim.* B **12**: 19–40.

SUCKLING, P.W. and J.E. HAY. 1976. The spatial variability of daily values of solar radiation for British Columbia and Alberta, Canada. *Climatol. Bull.* (McGill University). In press.

THEKAEKARA, M.P. and A.J. DRUMMOND. 1971. Standard values for the solar constant and its spectral components. *Nature Physical Sciences* **229**: 6–9.

WILSON, R.G. and D.E. PETZOLD. 1972. Daily solar radiation differences between stations in southern Canada: a preliminary analysis. *Climatol. Bull.* (McGill University) **11**: 15–22.

ACCESS TO STATION HISTORIES FOR STUDIES OF CLIMATIC CHANGE: AN APPEAL FOR IMPROVEMENT

A.J.W. Catchpole and C. Ponce
Department of Geography, University of Manitoba, Winnipeg

The mid-seventies are witnessing a surge in public concern with climatic change. Journalists, economists, and politicians are posing questions which, to them, appear to be simple and direct, and they expect the climatologist to respond with precise answers about climatic change. Of course, the climatologist is aware of a multitude of factors that obscure the nature of climatic change, and one such factor is the inhomogeneity of many long-term climatological records. As weather stations change their locality, as obstacles develop near instrument enclosures, or as instruments are replaced, repaired, or adjusted, so too the quality of climatological data changes. Consequently, all studies of long-term trends in climatic data should endeavour to discriminate between the real effects of climatic change and the effects of changes in the circumstances of observation.

This note refers to an attempt to survey the history of observational practices within a network of widely scattered stations in Canada. The survey procedure was predicated on the assumption that at each station there would be on file dates of change in location of the station, dates of re-siting of instruments within the station, dates when inspection detected faulty instrument exposure, dates when instruments were replaced, repaired, or adjusted, and dates when inspection detected faulty instrumentation. It was assumed that it would be a simple matter to retrieve this information from the station files and that the survey could be conducted by correspondence. The results of this survey are disappointing since they indicate that crucial historical information cannot easily be obtained.

This survey was associated with a study of long-term variations of total annual bright sunshine measured by the Campbell-Stokes sunshine recorder at 19 Canadian stations. Changes in station location and site conditions can seriously affect the performance of this instrument. The Canadian Atmospheric Environment Service publishes an Annual Meteorological Summary for selected stations and this summary contains a general station history. A scrutiny of these histories indicated that they generally contain insufficient data for the purposes of this research. The information sought in this survey was solicited in a letter that outlined the objectives of the research and requested information on the history of sunshine duration observations at each station. At first sight, it appeared that little comparative information could be extracted from the 19

Table 1. Classification and distribution of information in letters from each station. The stations are arranged roughly according to the nature of their responses. In alphabetical order, the stations are: Calgary Int. A., Dauphin A., Edmonton Ind. A., Harrow CDA, Kamloops A., Lethbridge CDA, London A., Medicine Hat A., New Liskeard, Oak Ridges, Ottawa CDA, Prince George A., Prince Rupert A., Regina A., Saskatoon SRC, Swift Current A., Toronto, Turbine, Victoria Gonzales Hts.

CONTENTS OF LETTERS			STATIONS																		
			1	2	3	4	5	6	7	8	9	10	11	12	13	14	15	16	17	18	19
Information Requested	Dated Change	date of change in instrumentation	√	√	√	√	√	√	√	√											
		date of change in location or site conditions	√	√	√	√					√	√	√	√							
		date of inspection of instrumentation or site	√				√	√						√				√			
	Undated Change	undated change in site conditions, location or instrumentation	√									√			√	√	√				
	Uniform Practices	instrumental conditions have not changed													√						
		location and site conditions have not changed																√			
Qualifying Advice		information derived partly from personal recollection or verbal communications		√	√				√	√	√		√		√	√			√		
		files are incomplete or non-existent at recording station		√		√					√						√			√	
Comments Advising Alternative Approaches to Problem		this information can be obtained from historical descriptions in Annual Meteorological Summaries													√		√				√
		this request should be directed elsewhere		√												√					
		these data are reliable and the question is unnecessary																	√		√

replies. They varied greatly in length, detail, and focus of interest. However, a systematic analysis of the replies allowed broad comparisons to be made between them, the results of which are given in Table 1. This table contains a classification of the different types of statements that appear in the letters and it indicates which of these classes occur in each letter.

The first six classes of statements embrace the information that was solicited. One of these classes is an undated statement that circumstances of observation had changed. This is useful information since it warns of a loss of homogeneity, but it is much less valuable than a dated class. Only 12 letters gave actual dates when location, site conditions, or instrumentation changed. Three of the remaining letters stated that changes had occurred without dating these. The seventh and eighth classes in Table 1 were statements intended to qualify the use of the information contained in the letters. Thus, 9 of the letters advised that this information was based wholly or partly on personal recollection or verbal communication, and 5 letters warned that the relevant files are incomplete or non-existent at the recording station. It is significant that 7 of the 12 letters containing dated information provided this qualifying advice. The final three classes in Table 1 advise the questioner that the information requested should be sought elsewhere, or that it is inappropriate to ask these questions. Three letters referred the questioner to the historical descriptions in the relevant Annual Meteorological Summary, one gave an alternative address, and two stated, or implied, that the question was unnecessary. One of the last two stated that site conditions and instrument changes do not affect the quality of sunshine duration data, and the second implied that the stringent inspections of the Amospheric Environment Service assure the homogeneity of meteorological data.

The results of this analysis indicate that the station records of sunshine duration, as currently kept, do not provide a totally reliable guide to the history of the observations of these data. It is also clear from the letters that most respondents fully understood the significance of the questions put to them and have made substantial efforts to supply the information requested. Since this information is not, in most cases, easily retrievable from station files, this note recommends that precise information on station histories should be maintained and be readily available to researchers investigating climatic change.

The current observational practices are undoubtedly adequate to detect and measure spatial variations of climate at the global and continental scales, and weather variations over short time periods. However, the amplitudes with which each of these vary are usually great in comparison to the amplitude of long-term climatic change. It is for this reason that an appeal is made for more sensitive practices to be developed for the monitoring of climatic change.

WEATHER IN THE WEST. Bette Roda Anderson. American West Publishing Company, Palo Alto, California, 223 pp. Distributed in Canada by John Wiley & Sons Canada Ltd, Rexdale, Ontario. $21.25

Belying its outward appearance, *Weather in the West* is much more than a coffee-table ornament. Its pages are slick and filled with ravishing pictures, but the text of this handsome, oversize volume is equally creditable. Published as part of a series on the Great West, its purpose is to provide an understanding of the weather and climates of the western half of the United States. In successfully achieving this purpose, the book serves as a fine introduction to meteorology and climatology.

Though its focus is the West, the book is not at all parochial in outlook. Sections are included on the sun, clouds, paleoclimates, forecasting, urban climatology, atmospheric optics, and cloud seeding in addition to those devoted more specifically to the different weather and climatic regimes of the American West. Even if it were devoted entirely to western climates, this would not be too severe a constraint because, as the author explains:

> Nearly every type of climate that occurs in the world's temperate zones can be found somewhere in the American West. This is hardly surprising, for the area covered in this book has a land mass as great as all of Europe outside the Soviet Union. It ranges from subtropical desert at its southern limits to arctic-like tundra on its mountain peaks. And it stretches two thousand miles east from a foggy seacoast to the deep heart of the North American continent.

The author confronts her subject with zest and writes with flair. Any reviewer would be tempted to quote passages at length. One more will have to suffice, from the preface to a group of chapters called The Weather Machine:

> Of all the ingredients that combine to make weather, sun is the sultan, the only energy source powerful enough to cause the endless variety of our skies. Nearly everything relates eventually to it: clouds, winds, precipitation patterns around the globe—everything except the seasons; they ebb and flow because of a simple accident of nature that the earth is tilted first toward then away from the sun.

Technical subjects are treated non-mathematically but almost always accurately. The author does not avoid such difficult and controversial topics as climate change and weather modification, but presents them fairly and with well judged balance.

Adding interest to the book are sections on the history of settlement in the West and the history of meteorology itself. Anecdotes, fact, and folklore about early settlers and their reaction to the weather are liberally included in the chapters on particular regions. The book ends with a glossary of meteorological terms and a thoughtfully arranged and thorough reading list.

This volume is a splendid layman's guide to western weather and should serve to introduce younger readers to the fascination of atmospheric science. Even the professional meteorologist should find the book interesting, especially if he needs to be reminded of the power of meteorological forces in shaping not only the physical environment, but social patterns as well.

R.R. Rogers
McGill University
Montreal

Figures in italics refer to 10th Annual Congress Issue

Section A: Index of Contributions by Author

Section B: CMS Subject Index

Section C: General Subject Index

INFORMATION FOR AUTHORS

Editorial policy. *Atmosphere* is a medium for the publication of the results of original research, survey articles, essays and book reviews in all fields of atmospheric science. It is published quarterly by the CMS with the aid of a grant from the Canadian Government. Articles may be in either English or French. Contributors need not be members of the CMS nor need they be Canadian; foreign contributions are welcomed. All contributions will be subject to a critical review before acceptance. Because of space limitations articles should not exceed 16 printed pages and preferably should be shorter.

Manuscripts should be submitted to: *Atmosphere*, Dept. of Meteorology, McGill University, 805 Sherbrooke St W., Montreal, Quebec, H3A 2K6. Three copies should be submitted, typewritten with double spacing and wide margins. Heading and sub-headings should be clearly designated. A concise, relevant and substantial abstract is required.

Tables should be prepared on separate sheets, each with concise headings.

Figures should be provided in the form of three copies of an original which should be retained by the author for later revision if required. A list of legends should be typed separately. Labelling should be made in generous size so that characters after reduction are easy to read. Line drawings should be drafted with India ink at least twice the final size on white paper or tracing cloth. Photographs (halftones) should be gloosy prints at least twice the final size.

Units. The International System (SI) of metric units is preferred. Units should be abbreviated only if accompanied by numerals, e.g., "10 m," but "several metres."

Footnotes to the text should be avoided.

Literature citations should be indicated in the text by author and date. The list of references should be arranged alphabetically by author, and chronologically for each author, if necessary.

RENSEIGNEMENTS POUR LES AUTEURS

Politique édirotiale. *Atmosphère* est un organe de publication de résultats de recherche originale, d'articles sommaires, d'essais et de critiques dans tous les domaines des sciences de l'atmosphère. Il est publié par la SMC à l'aide d'une subvention accordée par le gouvernement canadien. Les articles peuvent être en anglais ou en français. Il n'est pas nécessaire que les auteurs soient membre de la SMC; les contributions étrangères sont les bienvenues. A cause des limitations d'espace les articles ne doivent pas dépasser 16 pages dans le format final. Tout article sera soumis à un critique indépendant avant d'être accepté.

Les manuscrits doivent être envoyés à: *Atmosphère*, Dép. de météorologie, L'Université McGill, 805 Sherbrooke O., Montréal, Québec, H3A 2K6. Ils doivent être soumis en trois exemplaires dactylographiés à doubles interlignes avec de larges marges. Les titres et sous-titres doivent être clairement indiqués. Chaque article doit comporter un résumé qui soit concis, pertinent et substantiel.

Les tableaux doivent être préparés et présentés séparément accompagnés d'un titre concis et d'un numéro.

Les graphiques doivent être présentés en trois copies dont les originaux devraient être conservés par l'auteur au cas où ils seraient nécessaire de les reviser. Une liste des légendes des graphiques doit être dactylographiée séparément. L'étiquettage doit être de grand format de façon à ce qu'il soit facilement lisible après réduction du format. Le traçage des lignes doit s'effectuer au moyen d'encre de chine en doublant, au moins, le format final, le tout sur papier blanc ou sur papier à calquer et identifié adéquatement. Les photographies (demi-teintes) devraient être présentées sur épreuves glacées au double du format final.

Les unités. Le Système International (SI) d'unités métriques est préférable. Les unités devraient être abrégées seulement lorsqu'elles sont accompagnées de nombres, ex: "10m," mais "plusieurs mètres."

Les notes de renvoie au texte doivent être évitées.

Les citations littéraires doivent être indiquées dans le texte selon l'auteur et la date. La liste des références doit être présentée dans l'ordre alphabétique, par auteur et, si nécessaire, dans l'ordre chronologique pour chaque auteur.

The Canadian Meteorological Society / La Société météorologique du Canada

The Canadian Meteorological Society came into being on January 1, 1967, replacing the Canadian Branch of the Royal Meteorological Society, which had been established in 1940. The Society exists for the advancement of Meteorology, and membership is open to persons and organizations having an interest in Meteorology. At nine local centres of the Society, meetings are held on subjects of meteorological interest. *Atmosphere* as the scientific journal of the CMS is distributed free to all members. Each spring an annual congress is convened to serve as the National Meteorological Congress.

Correspondence regarding Society affairs should be directed to the Corresponding Secretary, Canadian Meteorological Society, c/o Dept. of Geography, Simon Fraser University, Burnaby 2, B.C.

There are three types of membership – Member, Student Member and Sustaining Member. For 1977 the dues are $20.00, $5.00 and $60.00 (min.), respectively. The annual Institutional subscription rate for *Atmosphere* is $15.00.

Correspondence relating to CMS membership or to institutional subscriptions should be directed to the University of Toronto Press, Journals Department, 5201 Dufferin St., Downsview, Ontario, Canada, M3H 5T8. Cheques should be made payable to the University of Toronto Press.

La Société météorologique du Canada a été fondée le 1er janvier 1967, en replacement de la Division canadienne de la Société royale de météorologie, établie en 1940. Cette société existe pour le progrès de la météorologie et toute personne ou organisation qui s'intéresse à la météorologie peut en faire partie. Aux neuf centres locaux de la Société, on peut y faire des conférences sur divers sujets d'intérêt météorologique. *Atmosphère*, la revue scientifique de la SMC, est distribuée gratuitement à tous les membres. A chaque printemps, la Société organise un congrès qui sert de Congrès national de météorologie.

Toute correspondance concernant les activités de la Société devrait être adressée au Secrétaire-correspondant, Société météorologique du Canada, Département de Géographie, L'Université Simon Fraser, Burnaby 2, B.C.

Il y a trois types de membres: Membre, Membre-étudiant, et Membre de soutien. La cotisation pour 1977 est de $20.00, $5.00 et $60.00 (min.) respectivement. Les institutions peuvent souscrire à *Atmosphère* au coût de $15.00 par année.

La correspondance concernant les souscriptions à la SMC ou les souscriptions des institutions doit être envoyée aux Presses de l'Université de Toronto, Département des périodiques, 5201 rue Dufferin, Downsview, Ontario, Canada, M3H 5T8. Les chèques doivent être payables aux Presses de l'Université de Toronto.